Long-term spatial and temporal microbial community dynamics in a large-scale drinking water distribution system with multiple disinfectant regimes.

Sarah Potgieter[a], Ameet Pinto[b], Makhosazana Sigudu[c], Hein du Preez [c], Esper Ncube[c], Stephanus Venter[a*]

[a] Department of Microbiology and Plant Pathology, University of Pretoria, Pretoria, South Africa

[b] Department of Civil and Environmental Engineering, Northeastern University, Boston, USA

[c] Scientific Services, Rand Water, Vereeniging, South Africa

*corresponding author: Stephanus Venter

Email address: fanus.venter@up.ac.za

Abstract

Long-term spatial-temporal investigations of microbial dynamics in full-scale drinking water distribution systems are scarce. These investigations can reveal the process, infrastructure, and environmental factors that influence the microbial community, offering opportunities to re-think microbial management in drinking water systems. Often, these insights are missed or are unreliable in short-term studies, which are impacted by stochastic variabilities inherent to large full-scale systems. In this two-year study, we investigated the spatial and temporal dynamics of the microbial community in a large, full scale South African drinking water distribution system that uses three successive disinfection strategies (i.e. chlorination, chloramination and hypochlorination). Monthly bulk water samples were collected from the outlet of the treatment plant and from 17 points in the distribution system spanning nearly 150 kilometres and the bacterial community composition was characterised by Illumina MiSeq sequencing of the V4 hypervariable region of the 16S rRNA gene. Like previous studies, *Alpha-* and *Betaproteobacteria* dominated the drinking water bacterial communities, with an increase in *Betaproteobacteria* post-chloramination. In contrast with previous reports, the observed richness, diversity, and evenness of the bacterial communities were higher in the winter months as opposed to the summer months in this study. In addition to temperature effects, the seasonal variations were also likely to be influenced by changes in average water age in the distribution system and corresponding changes in disinfectant residual concentrations. Spatial dynamics of the bacterial communities indicated distance decay, with bacterial communities becoming increasingly dissimilar with increasing distance between sampling locations. These spatial effects dampened the temporal changes in bulk water community and were the dominant factor when considering the entire distribution system. However, temporal variations were consistently stronger as compared to spatial changes at a individual sampling location and demonstrated seasonality. This study emphasises the need for long-term studies to comprehensively understand the temporal patterns that would otherwise be missed in short-term investigations. Furthermore, systematic long-term investigations are particularly critical towards determining the impact of changes in source water quality, environmental conditions, and process operations on the changes in microbial community composition in the drinking water distribution system.

Keywords

Drinking water distribution systems; Bulk water; Disinfection; Microbial community ecology; Long-term investigation; Temporal and spatial dynamics.

Highlights

- Long-term sampling campaign within a large-scale drinking water distribution system with multiple disinfectant regimes.
- Strong temporal trends in alpha diversity correlated with temperature changes.
- Temporal trends were dominant at individual sample sites and indicated seasonal variations.
- Temporal dynamics were less pronounced as bulk water moved farther away from the treatment plant.
- Spatial dynamics were stronger than temporal dynamics when considering the distribution system as a whole.

Abbreviations

DWDS, drinking water distribution system; DWTP, drinking water treatment plant; OTU, operational taxonomic unit; AMOVA, analysis of molecular variance; PERMANOVA, permutational analysis of variance; MRA, mean relative abundance; PCoA, Principal coordinate analysis.

1. Introduction

Drinking water distribution systems (DWDSs) are designed and maintained to transport chemically and biologically safe, potable water to the consumers. These systems are complex aquatic environments with multiple ecological niches that support microbial growth through the different stages of the DWDS. The microbial ecology of DWDSs is governed by environmental and engineering factors as well as operational conditions that influence the composition and structure of bacterial communities present in the biofilms, bulk water and sediments (Liu *et al.,* 2013; Prest *et al*., 2016a; Liu *et al*., 2017). Despite disinfection during water treatment, microorganisms grow during distribution with reported microbial cell numbers ranging between 10^4 – 10^6 cells per litre (Hammes *et al*., 2008). This persistent microbial community can be highly diverse including bacteria, archaea, free living amoebae, fungi and viruses (You *et al*., 2009; Thomas and Ashbolt, 2011; Siqueira and Lima, 2013; Liu *et al.,* 2013; Gall *et al*., 2015).

The concentration and composition of microorganisms within DWDSs is influenced by multiple treatment processes, specifically primary and secondary disinfection through the use of chlorine and/or chloramine dosing, respectively (Gomez-Alvarez *et al*., 2012). This final step of drinking water treatment profoundly alters the DWDS microbiome structure and composition and significantly reduces bacterial cell numbers depending on the disinfectant used (Proctor and Hammes, 2015; Prest *et al*., 2016a). However, despite disinfection, DWDS microbial communities persist in a limited, low-nutrient environment and disinfection may even select for unwanted bacteria such as *Mycobacteria*, ammonia- and nitrite-oxidising bacteria (Proctor and Hammes, 2015).

The bulk water is the primary medium for the spread of microorganisms, nutrients, and particles throughout the DWDS and it feeds into the point-of-use (PoU), which is the final point of consumer exposure to the drinking water microbiome (Liu *et al.,* 2013; Bautista-de los Santos *et al*., 2016). It has long been assumed that bacteria in the bulk water originate from detachment of biofilms or re-suspension of the sediments rather than bacterial growth in the bulk phase itself (Prest *et al*., 2016a). However, microbial communities within biofilms and bulk water have been shown to be distinct and biofilms from DWDS pipe walls may only have

a minor impact on the microbial community in the bulk water at the point of consumption (Henne *et al*., 2012; Liu *et al.,* 2014). Bulk water communities have been found to be spatially stable over short time scales irrespective of the DWDS sample location (Lautenschlager *et al*., 2013; Roeselers *et al.,* 2015) and have also been reported to display annually reproducible temporal trends (Pinto *et al*., 2014).

Due to developments in high throughput sequencing, our understanding of the DWDS microbiome has significantly improved (Proctor and Hammes, 2015; Bautista-de los Santos *et al*., 2016). Several studies have highlighted the effects of specific characteristics on the dynamics of microbial communities, including different treatment strategies (Gomez-Alvares *et al*., 2012; Hwang *et al*., 2012; Wang *et al*., 2014b, Bautista-de los Santos *et al*., 2016), distribution (Nescerecka *et al*., 2014; Shaw *et al*., 2015), process operations (Pinto *et al*., 2012; Lautenschlager *et al*., 2014; Wu *et al*., 2015), hydraulic conditions (Douterelo *et al*., 2014), water age and residence time (Wang *et al*., 2014a; Prest *et al.,* 2016a; Zlatanovic *et al*., 2017) as well as pipe material (Niquette *et al*., 2000; Wang *et al*., 2014a).

Although seasonal changes in DWDS microbial communities have previously been investigated (McCoy and VanBriesen, 2012 and 2014; Pinto *et al*., 2014; Ling *et al*., 2016; Zlatanovic *et al*., 2017), long-term, in-depth investigations of spatial and temporal dynamics of DWDS microbial communities are rare. Temporal dynamics of DWDSs cannot be accurately described without an extensive, long-term and high-frequency sampling strategy (Prest *et al*., 2016b). Such long-term investigations can provide insight into robust processes, infrastructure, and environmental factors (i.e. temperature, pH, disinfectant residuals, turbidity, etc.) that influence the microbial community, presenting opportunities to re-think the management of microbial growth and community composition in drinking water systems. Often, these insights into seasonal variations are unreliable in short-term or low sampling frequency studies due to the stochastic variabilities inherent to large full-scale systems. Short term or single time point sampling cannot be extrapolated to represent other times of the year, as several studies have shown bacterial communities can undergo significant temporal variations even within a single year (Pinto *et al*., 2014; Prest *et al* 2016b).

The primary challenge in terms of defining the drinking water microbiome is that it changes dynamically through all stages of the DWDS. The DWDS represents a microbial continuum, where the given volume of water and associated microbial community migrates while being influenced by changing disinfectant residual concentrations, nutrient bio-availability, and by the microbial communities in the biofilms and sediments. Therefore, an integral component of this study was to assess how spatial-temporal variation shapes the drinking water microbial community as it traverses through varying disinfection regimes (Proctor and Hammes, 2015). The current study aims to understand how the temporal and spatial dynamics of a unique and complex large-scale drinking water distribution network shapes the bacterial community structure and composition. To this end, a two year sampling campaign was conducted for a complex and multiple branching section of the DWDS that encompasses a three-stage disinfectant strategy i.e. initial chlorine dosing followed by the addition of chloramine and lastly, hypochlorite. The objectives were to: (i) assess long-term seasonal variations in the bacterial community of the DWDS over two years, (ii) determine the effects of the spatial configuration of DWDS on the bacterial community, considering the use of three different disinfectant residuals, and (iii) to understand the interplay between the temporal and spatial dynamics within the DWDS as a whole as well as within each disinfection strategy. This long-term study aims to provide a unique insight into physical-chemical factors impacting the spatial-temporal dynamics of the drinking water microbiome in the DWDS with multiple disinfectant regimes. This knowledge combined with previous (and future) spatial-temporal studies may help water utilities identify strategies to manage the drinking water microbiome in the DWDS to ensure its safety and stability.

2. Methodology

2.1 Site description and sample collection

Sampling was conducted at the outlet of a South African full-scale drinking water treatment plant (DWTP) and corresponding DWDS, from October 2014 to September 2016. In its entirety, this water utility serves consumers over a vast network, stretching over 3056 kilometres covering 18,000 km^2. The DWDS feeds 58 service reservoirs which supply large metropolitan and local municipalities as well as mines and industries with on average, 3653 million litres of water supplied daily to approximately 11 million people. Due to the

complexity, multiple distribution branches and vastness of this DWDS, a section of the distribution system was selected for this study, originating from the DWTP and spanning approximately 150 km of the corresponding DWDS pipeline.

Treatment of source water derived from surface water consists of coagulation with polymeric coagulants, flocculation and addition of lime (55-70 mg/L calcium hydroxide), sedimentation, pH adjustment with CO_2 gas followed by filtration (rapid gravity sand filters) and finally disinfection, which includes 3 disinfection strategies. First, the filter effluent is dosed with chlorine where liquid chlorine is evaporated and bubbled into carriage water to be dosed into the main water for disinfection. Chlorine dosages vary depending on the source water quality and the system demand, which is typically higher in the summer months. The total residual chlorine at these dosages varies between 1 mg/L in summer and 1.5 mg/L in winter after 20 minute contact time. Second, within this selected section of the DWDS, chlorinated water leaving the DWTP is again dosed with chloramine (0.8 to 1.5 mg/L) at a secondary disinfection boosting station approximately 23 km from the treatment plant. Here, monochloramine residuals vary on average between 0.8 mg/L in the autumn and 1.5mg/L in the spring. And finally, bulk water is again disinfected with hypochlorite at locations towards the end of the sampled DWDS section (approximately 120 km from the DWTP). In this hypochlorinated section of the DWDS, total residual chlorine varies on average between 0.6 mg/L in the summer and 1.2 mg/L in the winter. Free residual chlorine remains constant both temporally and spatially, varying on average between 0.3 and 0.2 mg/L. The dissolved organic carbon (DOC) concentrations in the DWDS were relatively constant throughout the duration of the study (i.e. between 3.5 and 4.2 mg Carbon/L, in autumn and spring, respectively). Further details on range of physical-chemical parameters, length, composition, and age of the pipe line sections connecting the DWDS sample locations were obtained from the utility for this study (Figure 1 and Table S4).

Bulk water samples were collected from 18 locations including the outlet of the DWTP, immediately before the chlorinated water enters the DWDS, and 17 locations within the DWDS (including bulk water samples from pipeline and reservoirs). This included 2 chlorinated, 13 chloraminated, and 3 hypochlorinated bulk water samples. Sampling occurred consecutively for 2 days on a monthly basis for 2 years, except for January 2016 and sample in July 2016 for

sample site CHM2.2, resulting in the collection of 413 samples. Sample site descriptions and DWDS layout are provided in Figure 1 and Table 1.

2.2 Sample processing

Bulk water samples were collected in 8L sterile Nalgene polycarbonate bottles and transported to the laboratory cold where they were kept at 4°C for 24 to 48 hours until filtered. Samples were filtered to harvest microbial cells by pumping the collected bulk water through STERIVEX™ GP 0.22 µm filter units (Millipore) using a Gilson® minipuls 3 peristaltic pump. Typically, 8L of bulk water were filtered for each sample. For samples collected directly after a disinfection, 16L of bulk water was filtered. The filters were kept in the dark and stored at -20°C until processing and DNA extraction. A traditional phenol/chloroform extraction method optimised by Pinto *et al.* (2012) was used for the isolation of DNA from cells immobilised on filter membranes. This protocol represents a modified version of the protocol described by Urakawa *et al.* (2010). Extracted DNA was sent to the Department of Microbiology and Immunology at the University of Michigan, Ann Arbor, USA for sequencing of the V4 hypervariable region of the 16S rRNA gene using the Illumina MiSeq platform. The dual-index paired-end sequencing approach, described by Kozich *et al.* (2013), resulted in paired reads with each read pair with a length of 250 nucleotides. All raw sequence data have been deposited with links to BioProject accession number PRJNA445682 in the NCBI BioProject database (https://www.ncbi.nlm.nih.gov/bioproject/).

2.3 Sequencing data processing

Due to unsuccessful sequencing attempts (i.e. failed DNA amplification), 65 of the 413 samples collected were excluded (excluded samples are described in Table S1) and the number of samples per sample site is indicated in Table 1. Failure of DNA amplification may have been a consequence of multiple factors i.e. low DNA concentrations, the potential presence of inhibitors (i.e. humic substances, phenolic compounds) and/or extensive DNA damage caused by high levels of disinfectant (i.e. chlorine) (Van Aken and Lin, 2011; Schrader *et al*., 2012). Sequence processing and analysis of the remaining 348 samples was performed using mothur (version 1.35.1) (Schloss et al., 2009) according to the protocol outlined previously (Kozich, et al., 2013). Merging of the forward and reverse reads yielded 11,568,699 sequences and

resulting sequences were screened by allowing a maximum length of 275 base pairs (bp) and minimum length of 250 bp. Sequences with more than eight homopolymers and any ambiguities were removed. Sequences were aligned to the SILVA reference database (Quast et al., 2013) and resulting alignments were trimmed using the filter.seqs option in mothur, ensuring that all sequences were aligned along similar regions of the V4 region of the 16S rRNA gene. The filtered and aligned sequences were further processed through the pre.cluster option by using a pseudo-single linkage algorithm with a 2-bp similarity threshold. Chimeras were identified using UCHIME (Edgar et al., 2011) and removed. The remaining 8,568,237 quality filtered sequences were classified using the Greengenes database (DeSantis et al., 2006), with a threshold confidence level of 80%. Sequences with an unknown domain level of taxonomy were discarded, resulting in a total of 8,314,324 sequences with an average of 23,892 ± 13,260 sequences per sample and the minimum and maximum number of sequences per sample being 1007 and 71843, respectively. Sequences were aligned using average neighbour algorithm into operational taxonomic units (OTUs) with a similarity cut-off of 97%.

2.4 Statistical analysis

Multivariate Cut-off Level Analysis, MultiCoLA (Gobet et al., 2010) was applied to evaluate the extent to which each OTU contributes structure of each community and filter the dataset to only retain OTUs that explained majority of the community structure variability. Specifically, the dataset was sorted according to the decreasing total sum of OTU sequences and then the top 1% of OTUs were retained, where each of the top 1% OTUs retained had a minimum of 3194 sequences. Mantel's test, was performed in R using the mantel function in the vegan package (Oksanen *et al*., 2015), was then performed between the structure based dissimilarity matrix constructed using the original dataset and one constructed using only the dataset consisting of the retained top 1% OTU dataset to determine whether the variability within the bacterial community structure was maintained within the smaller subset of OTUs.

Alpha-diversity indices (observed richness, Shannon Index, Inverse Simpson Index and Pielou's evenness) were calculated using the summary.single function in mothur (Schloss *et al*., 2009) incorporating the parameters, iters=1000 and subsampling=1007 (sample containing the least number of sequences). Good's coverage estimates were included to determine the

percentage of coverage associated with each sample after subsampling. Testing for normality using Shapiro-Wilk test and Q-Q plot, and Leven's test for homogeneity of variance revealed that alpha-diversity indices had a non-normal distribution, using the stats (R Core Team, 2015) and car (Fox and Weisberg, 2011) packages, respectively. Kruskal-Wallis one-way analysis of variance and post-hoc Dunn's test were performed in R using the stats and dunn.test (Dinno, 2017) packages, respectively to determine whether alpha-diversity indices were significantly different when grouped based on DWDS sample location, month, season or disinfectant used.

Beta-diversity analyses were performed to compare samples using OTU-level assignment (Jaccard and Bray-Curtis) and phylogenetic placement (weighted and unweighted UniFrac). Membership (Jaccard and unweighted UniFrac) and structure based (Bray-Curtis and weighted UniFrac) beta-diversity metrics were calculated using mothur (Schloss *et al*., 2009). Phylogenetic-based metrics were obtained by constructing a phylogenetic tree containing all sequences (97% similarity threshold), using the clearcut command in mothur (Evans *et al*., 2006; Lozupone *et al.,* 2011). All matrices were calculated after 1000 subsamplings of the entire data set (iters=1000) to the number of the least number of sequences (n = 1007) ensuring that all samples were compared with the same sequence depth. All four beta-diversity metrics and metadata files containing sample location, disinfection type, seasons and months were imported to R (http://www.R-project.org) for statistical analyses, including permutational analysis of variance (PERMANOVA) using the adonis function in the vegan package (Oksanen *et al*., 2015). Analysis of Molecular Variance (AMOVA) was performed in mothur, using the amova function, to determine the effect of different groupings of samples based on DWDS sample location, month, season and disinfection type (Excoffier, 1993; Anderson, 2001). Principal-coordinate analysis (PCoA) using Bray-Curtis and Jaccard distances were performed using the phyloseq package (McMurdie and Holmes, 2013). All plots were constructed using the ggplot2 package (Wickham, 2009).

3. Results

3.1 Small percentage of OTUs maintain the majority of the spatial and temporal trends

The bacterial community within all samples was taxonomically diverse with 9,516 OTUs being identified across all samples. Of the 99% low-abundance OTUs removed using MultiCoLA (Gobet *et al.,* 2010), 69.5% had total reads of 10 or less. Furthermore, of those OTUs removed, 14.4% were doubletons and 26.1% were singletons. The 95 OTUs (Table S2) that were retained constituted >1% of the total sequence counts and were shared among all sample points. These frequently detected 95 OTUs made up for 90% of the total sequences post quality filtering. Furthermore, these 95 OTUs captured 99% of spatial-temporal variability between samples (Mantel's $R_{Bray\text{-}Curtis} = 0.993$; $p = 0.001$). We also assessed the effect of subsampling, employed as means of normalizing variability in library size across samples, on the diversity captured within each sample based on Good's coverage analyses. This indicated that subsampling at a library size of 1007 sequences captured the majority of the richness for all samples (i.e., Good's coverage = 96.6 ± 0.6%).

3.2 Dominance of Alpha- and Betaproteobacteria varies depending on the type of disinfectant residual

The drinking water microbial community was dominated by bacteria (99.7% sequences were of bacterial origin), with archaea constituting only 0.3% of the total sequences. Of the 60 bacterial phyla identified, *Proteobacteria* was the most dominant across all samples with a mean relative abundance (MRA) of 78.2 ± 12.4%, constituting 82.4% of the total sequences (6,861,465 sequences) and 48 to 89% of the bacterial community in any given sample. The second most dominant phylum was *Planctomycetes* with a MRA of 10.1 ± 8.6%, constituting 7.7% of the total sequences (Table S3).

Further characterisation of the bacterial classes revealed *Alphaproteobacteria*, *Betaproteobacteria*, *Planctomycetia* and *Gammaproteobacteria* dominated, with MRAs of 49.6 ± 8.3%, 22.6 ± 12.2%, 8.8 ± 7.2% and 4.5 ± 2.4% across all sample locations, respectively

(Figure 2). *Betaproteobacteria* showed a significant increase in relative abundance following chloramination (MRA of 2.6 ± 3.1% in CHM1 to MRA of 37.8 ± 17.2% in CHM2). More specifically, members belonging to *Betaproteobacteria* (i.e. OTUs classified to the genus *Nitrosomonas* and the family *Nitrosomonadaceae*, the genus *Gallionella*) as well as members from the genus *Nitrospira,* increased after chloramination. However, some OTUs persisted after chloramination, including members of the phyla *Planctomycetes*, *Cyanobacteria* and the proteobacterial class *Alphaproteobacteria* (e.g. members of the genus *Hyphomicrobium*). *Alphaproteobacteria* remained relatively stable throughout the duration of the study, but showed a higher abundance in the summer months (MRA 52.9 ± 21.0%) compared to the winter months (MRA 44.7 ± 17.7%). Similarly, the relative abundance of *Betaproteobacteria* was highest in the summer months particularly within the chloraminated section of the DWDS (MRA 32.0 ± 21.0%) with a maximum MRA of 41.9 ± 25.4% in December 2015 but decreased in the spring (MRA 18.1 ± 17.8%). Conversely, the classes *Planctomycetia* and *Gammaproteobacteria* showed a decreased relative abundance in the summer months (MRA 5.4 ± 10.6% and MRA 1.7 ± 4.3%, respectively) to maximum relative abundance in the spring months (MRA 13.7 ± 12.5% and MRA 7.2 ± 13.5%, respectively). *Planctomycetia* also showed a decrease in relative abundance following chloramination and increased residence time in the reservoirs (CHM2) from a MRA of 22.4 ± 6.6% in samples before the reservoirs at CHM2 to a MRA of 6.5 ± 2.0% after the reservoirs. This decrease in *Planctomycetia* strongly correlated with an increase in *Betaproteobacteria* relative abundance (Pearson's R = -0.74, $p < 0.001$). Other bacterial classes with a MRA above 1% across all sample sites included the *Cyanobacterial* class 4C0d-2, *Nitrospira, Actinobacteria* and *Phycisphaerae* (MRA 2.0 ± 1.9%, 1.6 ± 2.0%, 1.4 ± 1.3% and 1.2 ± 1.6%, respectively). The remaining 140 classes and unclassified taxa constituted 9.9% of the total sequences with varying relative abundance throughout the year.

At the OTU level, the most abundant OTUs (overall contribution to abundance >1%) are shown in Table 2. The most abundant OTU was classified as *Nitrosomonas* (class: *Betaproteobacteria*, family: *Nitrosomonadaceae*) with MRA of 15.0 ± 18.9% and constituted 18.5% of the total sequences and had 100% sequence similarity to *Nitrosomonas oligotropha*. A significant increase in the relative abundance of *N. oligotropha*-like OTU was observed following chloramination and increased residence time in the reservoirs (from MRA 0.2 ± 0.4%

in CHM1 to MRA 18.8 ± 22.1% in CHM2). The relative abundance of OTUs classified as *Nitrosomonas* increased from 4-11% of the total betaproteobacterial sequences in chlorinated water (MRA 0.3 ± 0.8%) to 23-40% of betaproteobacterial sequences post chloramination (MRA 16.2 ± 19.3%). The relative abundance of four most abundant OTUs (55.4% of the total sequences) (Table 2) was strongly correlated with that of OTU 1 (Genus: *Nitrosomonas*) and OTU 2 (Order: *Rhizobiales*) which increased in relative abundance in the summer months, whereas OTU 3 (Order: *Rhizobiales*) and OTU 4 (Genus: *Sphingomonas*) which increased in relative abundance in the winter months. Specifically, *N. oligotropha*-like OTU reached its maximum abundance in the summer months (Dec - Feb) (MRA 25.3 ± 22.0% in summer compared to MRA 5.3 ± 11.5% in winter).

3.3 Increased richness in winter months with seasonal cycling

Alpha-diversity measures showed strong seasonal trends over the two years of this study. Richness (observed number of OTUs) was found to be higher in the winter months (July and August, average observed OTUs of 293 ± 161) compared to the summer months (December – February, average observed OTUs 207 ± 92) (Figure 3A). In the winter months, bacterial communities were also more diverse (average Shannon index winter: 3.00 ± 0.69 vs summer: 2.00 ± 0.70; average Inverse Simpson index winter: 10.04 ± 6.20 vs. summer: 5.26 ± 4.39) and even (average Pielou's evenness winter: 0.54 ± 0.12 vs. summer: 0.39 ± 0.13) (Figure S1).

Significant seasonal differences in the richness, diversity, and evenness of the bacterial community were observed (Kruskal-Wallis, $p < 0.05$). Post-hoc Dunn's test revealed significant differences between the summer and winter months (Bonferroni-corrected, $p < 0.05$ for all alpha-diversity measures). The changes in alpha-diversity measures correlated with seasonal temperature changes as well as varying chlorine (i.e. total and free chlorine) and monochloramine residuals within the DWDS. The increase in richness in the winter months showed a moderate negative correlation with water temperature (Pearson's $R = -0.56$, $p < 0.001$) (Figure 3B). Similar correlations were observed for Shannon diversity (Pearson's $R = -0.55$, $p < 0.001$), Inverse Simpson diversity (Pearson's $R = -0.46$, $p < 0.001$) and Pielou's evenness (Pearson's $R = -0.47$, $p < 0.001$). Conversely, richness showed a moderate positive correlation

with total chlorine (Pearson's $R = 0.48$, $p < 0.001$) and monochloramine (Pearson's $R = 0.48$, $p < 0.001$) (Fig. 3B and Table S4).

Seasonal trends were observed in bacterial community membership (Jaccard and unweighted UniFrac) and structure (Bray-Curtis and weighted UniFrac) across all sample locations, indicating that samples 6-7 months apart showed increased dissimilarity followed by a decrease in dissimilarity 11-12 months apart. However, these changes in dissimilarities were marginal suggesting relative temporal stability. These seasonal trends were more clearly reflected within the bacterial community structure (Bray-Curtis and weighted UniFrac) at individual sample sites. Specifically, reservoirs (CHM2.1, CHM5.2 and CHM5.3) and pipeline (CHM3.1-3.3, CHM4.1 and CHM4.2) samples sites within the chloraminated section of the DWDS showed significant seasonal trends with an increase in dissimilarity between samples 6 months apart (Bray-Curtis: 0.78 ± 0.19, weighted UniFrac: 0.53 ± 0.16) and a decrease in dissimilarity in samples 12 months apart (Bray-Curtis: 0.68 ± 0.19, weighted UniFrac: 0.43 ± 0.17).

Principal coordinate analysis (PCoA) based on Bray-Curtis distances revealed some seasonal cycling in community structure (Figure 4B). PCoA analyses using membership based Jaccard distances showed similar results (Figure S2). Although clustering was not pronounced and some overlap between seasons was observed, seasons from the first year clustered with the corresponding season of the following year, indicating seasonal cycling and suggested the potential for annual reproducibility in bacterial community membership and structure. More specifically, samples collected in summer and autumn clustered closer together, as well as those collected in spring and winter. These seasonal trends were more pronounced within the chloraminated (CHM) and hypochlorinated (HCHL) sections of the DWDS (Figure 4D and 4E, respectively). Though clear seasonal clustering was not observed for the chlorinated section of the DWDS, the data points clustered based on the year of sampling; more specifically samples from the second year clustered more closely together and distinct from the first years samples (Figure 4C). Differences were also observed in all beta-diversity metrics when samples were grouped based on the season in which they were collected, specifically between summer and winter (community membership [Jaccard and unweighted UniFrac: AMOVA, $F_{ST} \leq 3.98$, $p < 0.001$] and structure [Bray-Curtis and weighted UniFrac: AMOVA, $F_{ST} \leq 9.55$, $p < 0.001$]).

3.4 Increased temporal variation with increased distance from a disinfection point

The temporal variation was much more pronounced when considering individual sampling locations DWDS sample locations (Bray-Curtis, 0.72 ± 0.17 and weighted UniFrac, 0.52 ± 0.15) across the two year study period (Figure S3), as compared to the DWDS as a whole. On average, each sampling location showed 30-50% similarity in community structure between sampling time points. The bacterial community structure of sample locations immediately downstream of disinfection (i.e. CHL1, CHM1.1, CHM1.2 and HCHL1) showed minimal temporal variation. However, with increasing distance away from disinfection sites, particularly within the chloraminated section of the DWDS, samples sites showed increased temporal variation in community structure, particularly at the chloraminated reservoirs (CHM2 and CHM5) (Figure 5A and Figure S3). Similar trends in the temporal variation were also observed for community membership (Jaccard), however these were less pronounced (Figure 5B). The community membership was more dissimilar and the dissimilarity was less variable between temporal samples at each location (Jaccard; 0.78 ± 0.06 and unweighted UniFrac; 0.72 ± 0.05) with an average of only 20-30% similarity in community membership between sampling time points (Figure S3).

3.5 Significant distance decay in community structure with increasing distance between sample locations

Lower richness levels were observed for locations CHL1, CHL2 and CHM1 (observed OTUs: 137 ± 102, 101 ± 52 and 151 ± 52, respectively) (Figure S4), which corresponds to the location of these sample sites immediately after chlorination (CHL1) and immediately before and after chloramination (CHL2 and CHM1, respectively). Furthermore, these three locations showed significant differences in richness compared to the remaining DWDS sample locations (Dunn's test Bonferroni-corrected, $p < 0.05$). An increase in richness was observed within the chloraminated section of the DWDS, specifically following secondary disinfection at CHM1 (observed OTUs: 151 ± 52) and increased residence time in a reservoir at CHM4 (observed OTUs: 250 ± 106) (Fig. S4). The highest levels of richness were observed in the chloraminated reservoirs at CHM5, with an average observed OTUs of 303 ± 127. Significant differences in

the richness was observed when samples were grouped based on location (Kruskal-Wallis, $p < 0.05$). Further investigations revealed that these differences existed between locations before and after disinfection events, specifically after secondary disinfection with chloramine (Dunn's test Bonferroni-corrected $p < 0.05$ between CHM1 and CHM2), which correlated to the observed changes in richness. However this location based difference in richness was not observed for the other alpha diversity measures (Shannon Index, Inverse Simpson Index or Pielou's evenness, Kruskal-Wallis, $p > 0.05$).

Differences in microbial community structure were also observed following secondary disinfection with chloramine. PCoA ordination based on Bray-Curtis distances revealed limited spatial clustering within the community structure based on the different disinfection strategies (Figure 4A) with only chlorinated water samples (CHL1 and CHL2) clustered closer together. No clear clustering was observed for chloraminated or hypochlorinated samples. However, chlorinated samples were shown to be significantly different from samples containing the other two disinfectants (AMOVA, $F_{ST} \leq 9.18$, $p < 0.001$).

To assess the effect of distance between samples, the pairwise dissimilarity distances between individual samples were grouped based on the distance between them. The spatial dynamics of the bacterial community structure (Bray-Curtis and weighted UniFrac metrics) within the chloraminated section of the DWDS showed significant distance decay, with bacterial community structure becoming increasingly dissimilar with increasing distance between sampling locations ($R^2 = 0.14$, $p<0.001$) (Figure 6). However, no significant distance decay features were observed for community membership (Jaccard and unweighted UniFrac).

3.6 Dissimilarity between DWDS sample locations conforms to the layout of the DWDS

Beta diversity distances between samples immediately after disinfection and all other samples within each disinfection section were performed in line with the layout of the DWDS. The two chlorinated samples (CHL1 and CHL2) were on average 67% dissimilar. However, within the chloraminated section, clear spatial differences in community structure (Bray-Curtis and weighted UniFrac) were observed with samples from location CHM1 and CHM2 showing an

increase in dissimilarity. This correlated with the addition of chloramine at location CHM1 and increased residence in the reservoirs (CHM2.1 and CHM2.2). Dissimilarity in bacterial community structure decreased slightly in samples within chloraminated pipelines (locations CHM3 and CHM4) but again increased with chloraminated water entering the reservoirs at CHM5 (Figure 7). Samples within the hypochlorinated section showed decreased dissimilarity. This shows the variation in bacterial community structure (Bray-Curtis distances) as bulk water moves through the consecutive locations with an increase in dissimilarity at the reservoir sites. Similar variations in dissimilarity were observed with community membership (Jaccard and unweighted UniFrac), however the changes were marginal (Figure S5).

Furthermore, these variations in dissimilarity within each disinfection section correlate with changes in the disinfectant residual concentration, with both the chlorinated and chloraminated sections, demonstrating disinfectant decay. Within the chlorinated section the total chlorine decreased from 2.03 ± 0.14 mg/L in CHL1 to 0.97 ± 0.32 mg/L in CHL2. Within the chloraminated section both total chlorine and monochloramine concentrations decreased from location CHM1 to CHM5 (total residual chlorine: CHM1 2.20 ± 0.20 mg/L to CHM5 0.77 ± 0.62 mg/L; Monochloramine: CHM1 2.13 ± 0.30 mg/L to CHM5 0.66 ± 0.61 mg/L). Conversely, total residual chlorine concentrations remained relatively stable within the hypochlorinated section of the DWDS.

3.7 Temporal dynamics are dominant at a localised level

To further assess the impact of spatial and temporal dynamics on the bacterial community, samples were grouped based on season versus DWDS sample location and were compared using membership based (Jaccard and unweighted UniFrac) and structure based (Bray-Curtis and weighted UniFrac) metrics. PERMANOVA results (Table S5) of all four beta-diversity metrics showed that variations in the bacterial community over the DWDS as a whole, were best explained by sampling location (PERMANOVA, $R^2 \leq 0.21$) whereas, seasonal groupings had little or no impact on the DWDS bacterial community when considering all sample locations together (PERMANOVA, $R^2 \leq 0.07$).

Although the three disinfection sections did not cluster independently in the PCoA analyses (Figure 4A), when the bacterial communities were grouped based on the 3 disinfection strategies used and compared, the differences in community membership and structure were statistically significant (AMOVA, $F_{ST} \leq 10.92$, $p < 0.001$). This difference between PCoA and AMOVA analyses may emerge due to underlying temporal trends (Figure 4B). Specifically, the temporal variation in samples within disinfection strategy may be larger than the differences between samples grouped by disinfection strategies. Therefore, in order to clearly understand the interplay between the spatial and temporal dynamics of the microbial community, each disinfection section was analysed separately [i.e. section 1: chlorinated water (CHL), section 2: chloraminated water (CHM) and section 3: hypochlorinated water (HCHL)] (Figure 1)]. PERMANOVA tests on these three defined sections based on all four beta diversity metrics revealed that although spatial groupings may best explain the overall variability among samples, temporal/seasonal groupings best explained the variability within each disinfection section. More specifically, this was clearly observed for the chlorinated section (section 1; CHL), where temporal groupings were better supported (PERMANOVA, yearly seasons: $R^2 \leq 0.41$ vs sample site: $R^2 \leq 0.05$) (Table S6) over spatial/location groupings. Spatial groupings in the chlorinated section (CHL) explained very little of the variation (approximately 5%) with low significance but considering that this section included only two sample locations (CHL1 and CHL2) this result is not surprising. Similarly, the hypochlorinated section (section 3; HCHL) included only the 3 hypochlorinated locations (HCHL1 - HCHL3), however these sample locations were more spatially variable which was reflected in the PERMANOVA results (yearly seasons: $R^2 \leq 0.22$ vs sample site: $R^2 \leq 0.12$) (Table S8). Although, temporal groupings explained more of the variation in section 3 (HCHL), spatial groupings also had an effect on the bacterial community, specifically within community structure (Bray-Curtis and weighted UniFrac).

For the chloraminated section (section 2; CHM), the differences between temporal and spatial groupings were marginal and not well supported (Table S7). Temporal groupings explained more of the variation in bacterial community structure (PERMANOVA for Bray-Curtis and weighted UniFrac: $R^2 \leq 0.06$) with the effect of temporal groupings on community membership being insignificant. Conversely, spatial groupings explained slightly more of the variation in community membership (PERMANOVA, Jaccard and unweighted UniFrac $R^2 \leq 0.07$) and had

no significant effect on community structure. However, the combination of both temporal and spatial groupings explained up to 36% of the variation, although only significant for community membership (Jaccard and unweighted UniFrac). These results indicate that although seasonal groupings may explain more of the variation within each section, spatial groupings may have more of an impact on the variation between samples in section 2 (CHM) than in section 1 (CHL) and 3 (HCHL). This observation could in part be due to the fact that section 2 includes more samples with greater distances between them and therefore allows the spatial dynamics in the DWDS to have more of an impact on the bacterial community.

4. Discussion

This study represents the first long-term spatial-temporal investigation of microbial community dynamics in a large DWDS that utilizes multiple disinfectant regimes (i.e. chlorination, chloramination and hypochlorination). In doing so, we provide unique insights into how a microbial community responds to different disinfectants and their concentrations as it migrates through the DWDS at multiple time-points over two years. Further, the duration of the study and the length of the DWDS studied allows us for the first time to contextualize the importance of spatial compared to temporal variation. To our knowledge majority of spatial-temporal studies thus far have either been performed on smaller and/or for much shorter periods of time (McCoy and VanBriesen, 2012 and 2014; Pinto *et al*., 2014; Prest *et al*., 2016b; Zlatanovic *et al*., 2017).

4.1 Bacterial community composition

Consistent with previous studies, *Proteobacteria* dominated the bacterial community (Bautista-de los Santos *et al*., 2016). The phylum *Proteobacteria* and particularly the two classes *Alpha-* and *Betaproteobacteria* have been shown to be dominant in almost all DWDS studies published thus far. Many community composition studies have reported on variations in the dominance of these two classes depending on, but not limited to multiple factors, such as disinfection strategy (Gomez-Alvares *et al.,* 2012; Wang *et al*., 2014b) and seasonal variations (McCoy and VanBriesen, 2012 and 2014; Pinto *et al*., 2014; Prest *et al*., 2016b; Zlatanovic *et al*., 2017). DWDS bacterial communities are complex and vary across different DWDS as well as over time within a single DWDS (Proctor and Hammes, 2015). Some DWDSs show increased

spatial and temporal variation whereas others have demonstrated microbial communities that remain spatially and temporally stable (Lautenschlager *et al*., 2013; Roeselers *et al.,* 2015).

In this study, while temporal trends the *Alpha-* and *Betaproteobacteria* were apparent, they were not significant. While, seasonal variations between these proteobacterial classes have previously been reported (McCoy and VanBriesen, 2012 & 2014), it is important to note that the observed seasonal variations are also correlated to changes in disinfection residual concentrations and therefore should be considered in proper context when discussing observed temporal trends. Disinfectant dosing is often adjusted according to temperature shifts and therefore influences the microbial diversity (McCoy and VanBriesen, 2012). Temporal trends were more clearly reflected at an individual OTU level. The seasonal fluctuations in *Nitrosomonas*-like OTUs corresponded to potential increases in nitrification in the summer months, which correlated to increased temperatures and decreased chlorine residual levels.

While the bacterial community for the studies system was diverse, a small percentage of bacteria dominated the overall bacterial community. In this study, only 95 OTUs (~1% of all detected OTUs) had an overall relative abundance >1% and were shared across all samples over the course of the study and explained majority of the observed spatial-temporal variation. Gobet *et al*. (2010) demonstrated that ecological patterns were maintained after removal of 35-40% of rare sequences and beta diversity patterns were similar after denoising the data set, suggesting that the removal of rare sequences may be beneficial for data sets with a large fraction of singletons. This was found to be the case in the current study as the subset of 95 OTUs showed temporal and spatial trends similar to those observed when all OTUs were considered, suggesting that the subset of OTUs may be sufficient to explain the variation in community structure and composition. This finding is not uncommon as Pinto *et al*. (2014) demonstrated that despite observing a wide taxonomic diversity, the changes in bacterial community structure could be explained by only 5% of the OTUs.

4.2 Effects of DWDS configuration and disinfection on bacterial community structure and composition

This DWDS consists of a complex network of underground pipelines with many interconnections, multiple reservoirs, and three different disinfection strategies (chlorination, chloramination and hypochlorination). The predominantly steel pipelines stretching over large distances (pipe length ranging from 6 km to 74 km), differ in internal lining material (bitumen or cement), diameter (ranging from 47 to 210 cm), and age (ranging from 16 to 81 years). The DWDS bulk water community therefore varies due to exposure to different disinfectants and the spatial heterogeneity of the system itself, allowing potential regrowth and increased interaction with biofilms present on the pipeline surfaces at a localised level (Srinivasan *et al*., 2008). In light of the variability within these parameters, the spatial heterogeneity of the DWDS can significantly influence the bacterial community as it moves through the DWDS. However, it is difficult to separate the effect of a single parameter on the bacterial community in a full-scale DWDS. For example, Wang *et al*. (2014) reported on the combined effects of disinfectant, water age and pipe material creating different physicochemical conditions and ecological niches, which can then select and promote the growth of various microbes.

Despite the complexities of the system, we were able to show several key findings providing useful insights into the influence of the spatial structure of the DWDS on the bacterial community. Specifically, the spatial dynamics of the bacterial community conformed to the layout of the DWDS and the three disinfection strategies had a significant impact on the microbial community, particularly with the addition of the secondary disinfectant (chloramine). Together with increased retention time in a reservoir, chloramination caused a significant change in the bacterial community composition and structure. Although the impact of reservoirs on the microbial community is not fully understood, the observed change in the microbial community was more pronounced in the first reservoir samples. These changes may be due to extended contact time between the microbial community and chloramine residuals due to potentially longer retention times in the reservoir (Hoefel *et al*., 2005). However, we were not able to decouple the effect of disinfection versus residence time in the reservoirs. This increased contact time with disinfectant residuals within the reservoirs coupled with residual decay, potentially allows for increased microbial regrowth during stagnation periods, causing

shifts in abundances and in microbial community profiles (Lautenschlager *et al*., 2013). Furthermore, the observed change in community structure and membership correlated to the observed disinfectant decay within the chlorinated and chloraminated sections of the DWDS. However, more pronounced disinfectant decay was observed within the chloraminated section. Chloramine maintains extended disinfectant residuals, however within this section of the DWDS there are large distances between sample locations contributing to increased water age and disinfectant decay (Hoefel *et al*., 2005). In addition, the bacterial community displayed distance decay features with bacterial community structure becoming more dissimilar with an increase in distance between chloraminated sample locations. These findings may help in the modelling of the variability in the bacterial community as it moves away from the DWTP and through the DWDS (Schroeder *et al.,* 2015).

The effect of disinfection on the community composition has previously been reported, indicating that *Alphaproteobacteria* are typically dominant in both chlorinated and chloraminated water, whereas *Betaproteobacteria* were found to have increased abundance in chloraminated water as opposed to chlorinated water (Berry, 2006; Wang *et al*., 2014). This was consistent with the observed changes in *Alpha-* and *Betaproteobacteria* in this study. A change in the bacterial community was also associated with an increase in richness following chloramination. Here, Baron *et al*., (2014) suggests that through chloramination, a potential loss of a select few dominant groups allowed for growth of a greater number of other species. Primary disinfection processes (chlorination in this case) typically dramatically reduce the bacterial community thereby potentially creating the opportunity of surviving microorganisms to proliferate and exploit the available nutrient pool (Hammes *et al*., 2008; Prest *et al*., 2016a).

4.3 Long-term seasonal variations in microbial community

In contrast to other studies (McCoy and VanBriesen, 2014; Pinto *et al*., 2014), winter months showed an increase in richness (observed OTUs), diversity and evenness although, an increase in richness in the winter months was also observed by Hwang and colleagues (2012). This increase in richness may be a consequence of a decrease in dominance of certain OTUs in the winter months, allowing for an increased detection of sequences of medium abundance and/or rare OTUs. Here a decrease in temperature may have a similar effect as chloramination in the

reduction of dominant groups, allowing the detection and/or growth less dominant species. This decrease in dominance may also result in the observed increase in diversity and the OTUs being more evenly distributed. Gilbert *et al*., (2012) also observed this increase in richness in the winter months in marine microbial communities. Here the authors concluded that the observed seasonal changes in richness indicate that the most common and dominant bacterial taxa have temporally defined niches. Ling *et al*. (2016) also suggested that the observed seasonal variation influenced the dynamics of several core populations identified in DWDS biofilms and was main driver in the overall variation in the biofilm community.

Seasonal cycling was observed in the bacterial community structure and membership. However, the seasonal clustering observed by Pinto *et al.* (2014) was more well defined likely due to high variation in seasonal temperatures in Ann Arbor, Michigan USA and the change in the blend ratio of source waters (i.e. surface and ground water) in summer and winter. Significant seasonal variations were also observed by Prest *et al*. (2016b) in the Netherlands where seasonal temperatures vary by approximately 20 °C. Conversely, large temperature fluctuations rarely occur in South Africa and throughout the year and surface water is obtained from the same source. Despite this we did observe seasonal cycling, which could be a combination of temperature changes, changes in source water community composition, and changes in disinfectant residual concentrations over time. Temporal trends were, in fact, more clearly reflected within the bacterial community structure at individual sample points over the two years. Variability in community structure at each sample point over the duration of the study was considerable, specifically in the chloraminated section of the DWDS indicating a high level of temporal variation in bacterial community structure at a single sample location. This observed variability was largely due to the changes in abundance of dominant groups as similar trends were not clearly reflected in community membership.

Although small temporal trends were observed for community membership, the high level of dissimilarity in membership may be a consequence of the large number of rare OTUs, indicating that there is only a small percentage of shared membership at each location. In microbial ecology studies across a wide range of ecosystems, rare OTUs often contribute to a large proportion of the observed taxa. They represent a high diversity of bacterial and archaeal lineages and often explain the high levels of temporal variability in community membership

(Shade *et al*., 2014; El-Chakhtoura *et al*., 2015). Although the ecological roles of the rare organisms are not well understood, it has been suggested that they may contribute to the community stability. In response to an environmental change, i.e. water temperature or disinfectant residuals, these rare OTUs may act as a reservoir and act as potential microbial seedbank when conditions change (Shade *et al*., 2014; El-Chakhtoura *et al*., 2015).

4.4 The interplay between spatial and temporal dynamics of the DWDS

A combination of parameters need to be considered for a comprehensive understanding of the bacterial community in the bulk water. When considering the DWDS as a whole, spatial dynamics explained more of the variation. This is likely due to the complexity of the large full-scale system such as this, with multiple interconnections, reservoirs and different disinfection residuals. It was shown that the extent of temporal variation in bacterial community structure, at each location, decreased as the bulk water moved away from the DWTP and through the DWDS, suggesting that the temporal dynamics are dampened by the spatial heterogeneity of the DWDS and the impact of DWDS specific microbial communities (i.e., sediments, biofilms) on the bulk water. This was clearly observed in the chloraminated section of the DWDS, where the distances between points were further apart than in the chlorinated and hypochlorinated sections.

Furthermore, samples farther away from treatment showed an increase in richness and diversity. Similar observations were reported by El-Chakhtoura and colleagues (2015), where the bacterial community structure changed during distribution, resulting in increased richness in the network. The increase of bacterial richness during distribution may be associated with regrowth, particularly in large distribution systems where bulk water is transported over long distances. Microbial growth in drinking water has been observed in the form of higher particle counts and increased turbidity (Liu *et al*., 2016), higher cell counts (Hammes *et al*., 2008) and increase in the presence of indicator organisms in the final tap water compared to the water leaving the treatment plant (van der Wielen *et al*., 2016). The water leaving the treatment plant may therefore be impacted by the distribution system itself through processes such as pipe corrosion (Sun *et al.,* 2014), the detachment of biofilms (Chaves Simões and Simões, 2013) and suspension of loose deposits (Liu *et al*., 2013; Liu *et al*., 2017; Liu *et al*., 2018). These

processes together in combination with increasing contact time with the disinfectant may explain the observed spatial dissimilarity observed in the bacterial community as bulk water moves away from the DWDP and through the DWDS.

At a more localised level, i.e., specific sample sites or sections, the temporal dynamics were clear and explained the variation as observed at individual sites/sections. This suggests that as the bulk water moves through the DWDS, the cumulative change in microbial community due to mechanisms ranging from growth, decay, sediment resuspension, and/or biofilm detachment is larger than the temporal change over a sampling frequency of this study (i.e., monthly). It is plausible that biofilms and/or sediments in the studied DWDS exhibit much higher temporal stability as compared to the bulk water and their seeding of the bulk water is the primary mechanism for the decreasing temporal variability with increasing DWDS distance from the DWTP.

5. Concluding remarks

Through conducting a long-term survey spanning two years, we were able to comprehensively characterise the temporal and spatial dynamics of the microbial community within a complex, large-scale DWDS. Here we show strong temporal trends in richness and diversity, correlated with seasonal changes in disinfectant residuals as well as seasonal cycling in the bacterial community structure and composition in the DWDS. Temporal trends were dominant at a localised level, showing seasonal variations, but when considering the DWDS in its entirety, spatial dynamics were stronger and explained more of the variation in the bacterial community structure. This study highlighted the interplay between the spatial and temporal dynamics of the DWDS. Here, temporal dynamics decreased as bulk water moved away from the treatment plant due to the potential seeding of the bulk water by the relatively temporally stable communities (i.e. biofilms and loose deposits) inherent to the DWDS. Complete understanding of the factors driving the changes in large-scale DWDS bacterial communities may be difficult to achieve as these DWDS are complex and inherently dynamic. However, through a long-term, high-frequency investigation such as this, we were able to clearly observe seasonal and annual patterns in the microbial community that would have otherwise been missed in a short-term study. Even though high diversity and variation was observed within the microbial

community, we detected a core community that was present in all samples collected as part of this study. This core community was able to tolerate a range of physical-chemical variations within the system, Therefore, this study contributes to current knowledge base in this field and provides the opportunity for drinking water utilities to understand the range of mechanisms that influence the bacterial community structure and composition, over varying temporal scales and/or operational stages.

Acknowledgements

This research was supported and funded by Rand Water, Gauteng, South Africa through the Rand water Chair in Water Microbiology at the University of Pretoria. Sarah Potgieter would also like to acknowledge the National Research Foundation (NRF) for additional funding. Furthermore, the authors would like to acknowledge the Centre for Microbial Systems Molecular Biology Lab, University of Michigan, USA for their services in Illumina MiSeq sequencing.

References

Anderson, M.J., 2001. A new method for non-parametric multivariate analysis of variance. Austral ecology 26 (1), pp.32-46.

Baron, J. L., Vikram, A., Duda, S., Stout, J. E and Bibby, K. 2014. Shift in the microbial ecology of a hospital hot water system following the introduction of an on-site monochloramine disinfection system. PLOS One 9 (7), e102679.

Bautista-de los Santos, Q. M., Schroeder, M. C., Sevillano-Rivera, M. C., Sungthong, R., Ijaz, U. Z., Sloan, W. T and Pinto, A. J. 2016. Emerging investigators series: microbial communities in full-scale drinking water distribution systems – a meta-analysis. Environmental Science: Water Research and Technology. doi: 10.1039/c6ew00030d.

Berry, D., Xi, C and Raskin, L. 2006. Microbial ecology of drinking water distribution systems. Current Opinion Biotechnology. 17: 297-302.

Chaves Simões, L and Simões, M. 2013. Biofilms in drinking water: problems and solutions. Rsc Advances. 3(8): 2520-2533.

Dinno, A. 2017. dunn.test: Dunn's Test of Multiple Comparisons Using Rank Sums. R package version 1.3.3. (http://CRAN.R-project.org/package=dunn.test).

DeSantis, T. Z., Hugenholtz, P., Larsen, N., Rojas, M., Brodie, E. L., Keller, K., Huber, T., Dalevi, D., Hu, P and Andersen, G. L. 2006. Greengenes, a Chimera-Checked 16S rRNA Gene Database and Workbench Compatible with ARB. Applied and Environmental Microbiology. 72: 5069-72.

Douterelo, I., Husband, S and Boxall, J. B. 2014. The bacterial composition of biomass recovered by flushing an operational drinking water distribution system. Water Research. 54: 100-114.

Edgar, R.C., Haas, B. J., Clemente, J. C., Quince, C and Knight, R. 2011. UCHIME improves sensitivity and speed of chimera detection. Bioinformatics. doi: 10.1093/bioinformatics/btr381.

El-Chakhtoura, J., Prest, E., Saikaly, P., van Loosdercht., Hammes, F and Vrouwenvedler, H. 2015. Dynamics of bacterial communities before and after distribution in a full-scale drinking water network. Water Research. 74: 180-190.

Evans, J., Sheneman, L and Foster, J. A. 2006. Relaxed Neighbour-Joining: A Fast Distance-Based Phylogenetic Tree Construction Method. Journal of Molecular Evolution. 62: 785-792.

Excoffier, L. 1993. Analysis of molecular variance (AMOVA) version 1.55. Genetics and Biometry Laboratory, University of Geneva, Switzerland.

Fox, J and Weisberg, S. 2011. An {R} Companion to Applied Regression, Second Edition. Thousand Oaks CA: Sage. URL:http://socserv.socsci.mcmaster.ca/jfox/Books/Companion

Gall, A. M., Mariñas, B. J., Lu, Y and Shisler, J. L. 2015. Waterborne Viruses: A Barrier to Safe Drinking Water. PLoS Pathogens. 11(6): e1004867. doi: 10.1371/journal.ppat.1004867.

Gilbert, J. A., Steele, J. A., Caporaso, J. G., Steinbrück., Reeder, J., Temperton, B., Huse, S., McHardy, A. C., Knight, R., Joint, I., Somerfield, P., Fuhrman, J. A and Field, D. 2012. Defining seasonal marine microbial community dynamics. The ISME Journal. 6: 298-308.

Gobet, A., Quince, C and Ramette, A. 2010. Multivariate cuttoff level analysis (MultiCoLA) of large community data sets. Nucleic Acids Research. 38(15): e155. doi:10.1093/nar/gkq545.

Gomez-Alvarez, V., Revetta, R. P and Santo Domingo, J. W. 2012. Metagenomic analysis of drinking water receiving different disinfection treatments. Applied and Environmental Microbiology. 78(17): 6095-6102.

Hammes, F., Berney, M., Wang, Y., Vital, M., Koster, O and Egli, T. 2008. Flow-cytometric total bacterial cell counts as a descriptive microbiological parameter for drinking water treatment processes. Water Research. 44(17): 4868-4877.

Henne, K., Kahisch, L., Brettar, I and Holfe, M. G. 2012. Analysis of structure and composition of bacterial core communities in mature drinking water biofilms and bulk water of a citywide network in Germany. Applied and Environmental Microbiology. 78(10): 3530-3538.

Hoefel, D., Monis, P. T., Grooby, W. L., Andrews, S and Saint, C .P. 2005. Culture-independent techniques for rapid detection of bacteria associated with the loss of chloramine residual in a drinking water system. Applied and environmental microbiology. 71(11): 6479-6488.

Hwang, C., Ling, F., Andersen, G. L., LeChevallier, M. W and Liu, W. 2012. Microbial community dynamics of an urban drinking water distribution system subjected to phases of chloramination and chlorination treatments. Applied and Environmental Microbiology. 78(22): 7856-7865.

Kozich, J. J., Westcott, S. L., Baxter, N. T., Highlander, S. K and Schloss, P. D. 2013. Development of a dual-index strategy and curation pipeline for analyzing amplicon-sequencing data on the MiSeq Illumina sequencing platform. Applied and Environmental Microbiology. 79: 5112-5120.

Lautenschlager, K., Hwang, C., Ling, F., Liu, W. T., Boon, N., Köster, O., Vrouwenvelder, H., Egli, T and Hammes, F. 2013. A microbiology-based multi-parametric approach towards assessing biological stability in drinking water distribution networks. Water Research. 47: 3015-3025.

Lautenschlager, K., Hwang, C., Ling, F., Liu, W. T., Boon, N., Köster, O., Egli, T and Hammes, F. 2014. Abundance and composition of indigenous bacterial communities in a multi-step biofiltration-based drinking water treatment. Water Research. 62: 40-52.

Lozupone, C., Lladser, M. E., Knights, D., Stombaugh, J. and Knight, R. 2011. UniFrac: an effective distance metric for microbial community comparison. The ISME journal. 5(2): 169-172.

Ling, F., Hwang, C., LeChevallier, M. W., Anderson, G. L and Liu, W-T. 2016. Core-satellite populations and seasonality of water meter biofilms in a metropolitan drinking water distribution system. ISME. 10: 582-595.

Liu, G., Verbeck, J. Q. J. C and Van Dijk, J. C. 2013. Bacteriology of drinking water distribution systems: an integral and multidimensional review. Applied and Environmental Microbiology. 97: 9265-9276.

Liu, G., Bakker, G. L., Vreeberg, J. H. G., Verberk, J. Q. J. C., Medama, G. J., Liu, M. C and Van Dijk, J. C. 2014. Pyrosequencing reveals bacterial communities in unchlorinated drinking water distribution system: An integral study of bulk water, suspended solids, loose deposits and pipe wall biofilm. Environmental Science and Technology. 48: 5467-5476.

Liu, G., Ling, F. Q., Van der Mark, E. J., Zhang, X. D., Knezev, A., Verberk, J. Q. J. C., Van der Meer, W. G. J., Medema, G. J., Liu, W. T. and Van Dijk, J. C. 2016. Comparison of particle-associated bacteria from a drinking water treatment plant and distribution reservoirs with different water sources. Scientific Reports. 6: 20367.

Liu, G., Zhang, Y., Knibbe, W-J., Feng, C., Liu, W., Medema, G and van der Meer, W. 2017. Potential impacts of changing water suppy-water quality on drinking water distribution: A review. Water Research. 116: 135-148.

Liu, G., Zhang, Y., Van der Mark, E., Magic-Knezev, A., Pinto, A., van den Bogert, B., Liu, W., Van der Meer, W and Medema, G. 2018. Assessing the origin of bacteria in tap water and distribution system in an unchlorinated drinking water system by SourceTracker using microbial community fingerprints. Water Research. 138: 86-96.

McCoy, S. T and VanBriesen, J. M. 2012. Temporal variability of bacterial diversity in a chlorinated drinking water distribution system. Journal of Environmental Engineering. 138(7): 786-795.

McCoy, S. T and VanBriesen, J. M. 2014. Comparing Spatial and Temporal Diversity of Bacteria in a Chlorinated Drinking Water Distribution System. Environmental Engineering Science. 31(1): 32-41.

McMurdie, P. J and Holmes, S. 2013. Phyloseq: An R package for reproducible interactive analysis and graphics of microbiome census data. PLoS ONE. 8(4): e61217.

Nescerecka, A., Rubulis, J., Vital, A., Juhna, T and Hammes, F. 2014. Biological instability in a chlorinated drinking water distribution system. PLOS One. 9(5): e96354.

Niquette, P., Servais, P and Savoir, R. 2000. Impacts of pipe materials on densities of fixed bacterial biomass in a drinking water distribution system. Water research. 34(6):1952-1956.

Oksanen, J., Guillaume Blanchet, F., Kindt, R., Legendre, P., Minchin, P. R., O'Hara, R. B., Simpson, G. L., Solymos, P., Stevens, H. H and Wagner, H. 2015. Vegan: Community Ecology Package. R package version 2.3-0. (http://CRAN.R-project.org/package=vegan).

Pinto, A. J., Xi, C and Raskin, L. 2012. Bacterial community structure in the drinking water microbiome is governed by filtration processes. Environmental Science and Technology. 46: 8851-8859.

Pinto, A., Schroeder, J., Lunn, M., Sloan, W and Raskin, L. 2014. Spatial-temporal survey and occupancy-abundance modelling to predict bacterial community dynamics in the drinking water microbiome. mBIO ASM. 5(3): e01135-14.

Prest, E. I., Hammes, F., van Loosdrecht, M. C. M and Vrouwenvelder, J. S. 2016a. Biological stability of drinking water: controlling factors, methods and challenges. Frontiers in Microbiology. 7(45): doi:10.3389/fmicb.2016.00045.

Prest, E. I., Weissbrodt, D. G., Hammes, F., van Loosdrecht, M. C. M and Vrouwenvelder, J. S. 2016b. Long-term bacterial dynamics in a full scale drinking water distribution system. PLoS ONE. DOI: 10.1371/journal.pone.0164445.

Proctor, C. R and Hammes, F. 2015. Drinking water microbiology – from measurement to management. Current Opinion in Microbiology. 33: 87-95.

Quast, C., Pruesse, E., Yilmaz, P., Gerken, J., Schweer, T., Yarza, P., Peplies, J and Glöckner, F. O. 2013. The SILVA ribosomal RNA gene database project: improved data processing and web-based tools. Nucleic Acids Research. 41(D1): D590-D596.

R Core Team 2015. R: A language and environment for statistical computing. R Foundation for Statistical Computing, Vienna, Austria. URL: http://www.R-project.org/.

Roeselers, G., Coolen, J., van der Wielen, P. W. J. J., Jaspers, M. C., Atsma, A., deGraaf, B and Schuren, F. 2015. Microbial biogeography of drinking water: patterns in phylogenetic diversity across space and time. Environmental Microbiology. 17(7): 2505-2514.

Schrader, C., Schielke, A., Ellerbroek, L and Johne, R. 2012. PCR inhibitors – occurrence, properties and removal. Journal of Applied Microbiology. 113: 1014-1026.

Schloss, P. D., Westcott, S. L., Ryabin, T., Hall, J. R., Hartmann, M., Hollister, E. B., Lesniewski, R. A., Oakley, B. B., Parks, D. H., Robinson, C. J and Sahl, J. W. 2009. Introducing mothur: open-source, platform-independent, community-supported software for describing and comparing microbial communities. Applied and environmental microbiology. 75(23): 7537-7541.

Schroeder, J. L., Lunn, M., Pinto, A. J., Raskin, L and Sloan, W. T. (2015). Probabilistic models to describe tge dynamics of migrating microbial communities. PLoS ONE. DOI:10.1371/journal.pone.0117221.

Shade, A., Jones, S. E., Caporaso, J. G., Handelsman, J., Knight, R., Fierer, N and Gilbert, J. A. 2014. Conditionally rare taxa disproportionately contribute to temporal changes in microbial diversity. mBio ASM. 5(4): 1-9.

Shaw, J. L. A., Monis, P., Weyrich, L. S., Sawade, E., Drikas, M and Cooper, A. J. 2015. Using amplicon sequencing to characterize and monitor bacterial diversity in drinking water distribution systems. Applied and environmental microbiology. 81(18): 6463-6473.

Siqueira, V. M and Lima, N. 2013. Biofilm formation by filamentous fungi recovered from a water system. Journal of Mycology. 1-9.

Srinivasan, S., Harrington, G. W., Xagoraraki, I and Goel, R. 2008. Factors affecting bulk to total bacteria ratio in drinking water distribution systems. Water Research. 42: 3393-33404.

Sun, H., Shi, B., Lytle, D. A., Bai, Y and Wang, D. 2014. Formation and release behaviour of iron corrosion products under the influence of bacterial communities in a simulated water distribution system. Environmental Science: Processes & Impacts. 16(3): 576-585.

Thomas, J. M and Ashbolt, N. J. 2011. Do Free-Living amoebae in treated drinking water systems present an emerging health risk? Environmental Science and Technology. 45(3): 860-869.

Urakawa, H., Martens-Habbena, W and Stahl, D. A. 2010. High abundance of ammonia-oxidising Archaea in coastal waters, determined by using a modified DNA extraction method. Applied and Environmental Microbiology. 76(7): 2129-2135.

Van Aken, B and Lin, L-S. 2011. Effect of the disinfection agents chlorine, UV irradiation, silver ions, and TiO_2 nanoparticles/near-UV on DNA molecules. Water Science and Technology. 64(6): 1226-1232.

van der Wielen, P. W. J. J., Bakker, G., Atsma, A., Lut, M., Roeselers, G and Graaf, B. D. (2016). A survey of indicator parameters to monitor regrowth in unchlorinated drinking water. Environmental Science: Water Research and Technology. 4(2): 683-692.

Wickham, H. 2009. ggplot2: Elegant Graphics for Data Analysis. Springer-Verlag New York, http://ggplot2.org.

Wang, H., Masters, S., Edwards, M. A, Falkinham, J. O and Pruden, A. 2014a. Effect of disinfectant, water age and pipe material on bacterial and eukaryotic community structure in drinking water biofilm. Environmental Science and Technology. 48: 1426-1435

Wang, H., Proctor, C. R., Edwards, M. A., Pryor, M., Santo Domingo, J. W., Ryu, H., Camper, A. K., Olson, A and Pruden, A. 2014b. Microbial community response to chlorine conversion in a chloraminated drinking water distribution system. Environmental Science and Technology. 48: 10624-10633.

Wu, H., Zhang, J., Mi, Z., Xie, S., Chen, C and Zhang, X. 2015. Biofilm bacterial communities in urban drinking water distribution systems transporting waters with different purification strategies. Environmental Biotechnology. 99: 1947-1955.

You, J., Das, A., Dolan, E. M and Hu, Z. 2009. Ammonia-oxidising archaea involved in nitrogen removal. Water Research. 43: 1801-1809.

Zlatanovic, Lj., van der Hoek, J. P and Vreeburg, J. H. G. 2017. An experimental study on the influence of water stagnation and temperature change on water quality in a full-scale domestic drinking water system. Water Research. 123: 761-772.

Figures

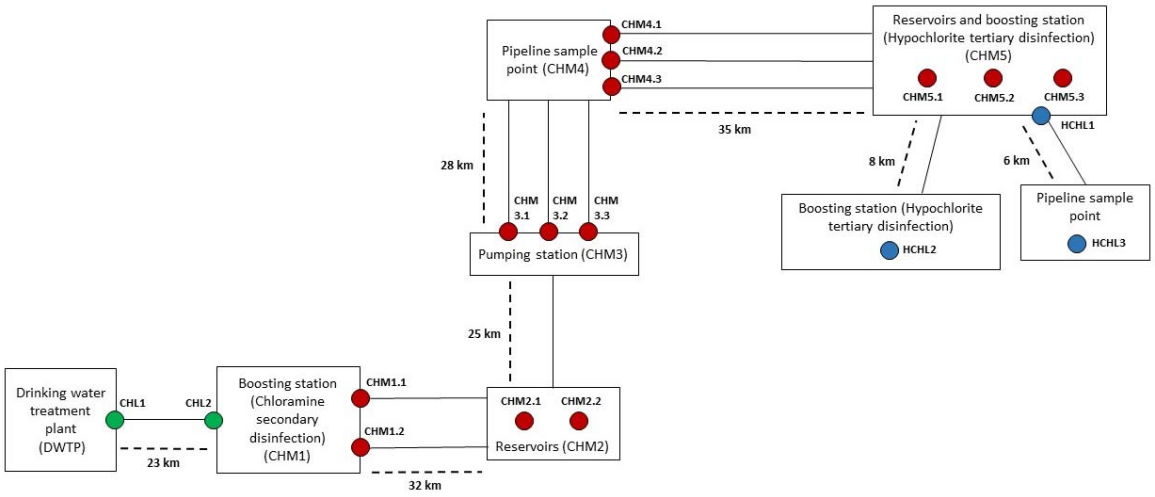

Figure 1. Schematic showing the layout of DWDS sample locations and respective sampling sites included in this study. Sample sites are indicated as circles and coloured according to the disinfectant residual used in that section of the DWDS [green circles, chlorine (CHL); red circles, chloramine (CHM) and blue circles, hypochlorite (HCHL)]. Dashed lines indicate the pipe distances (km) between sample locations.

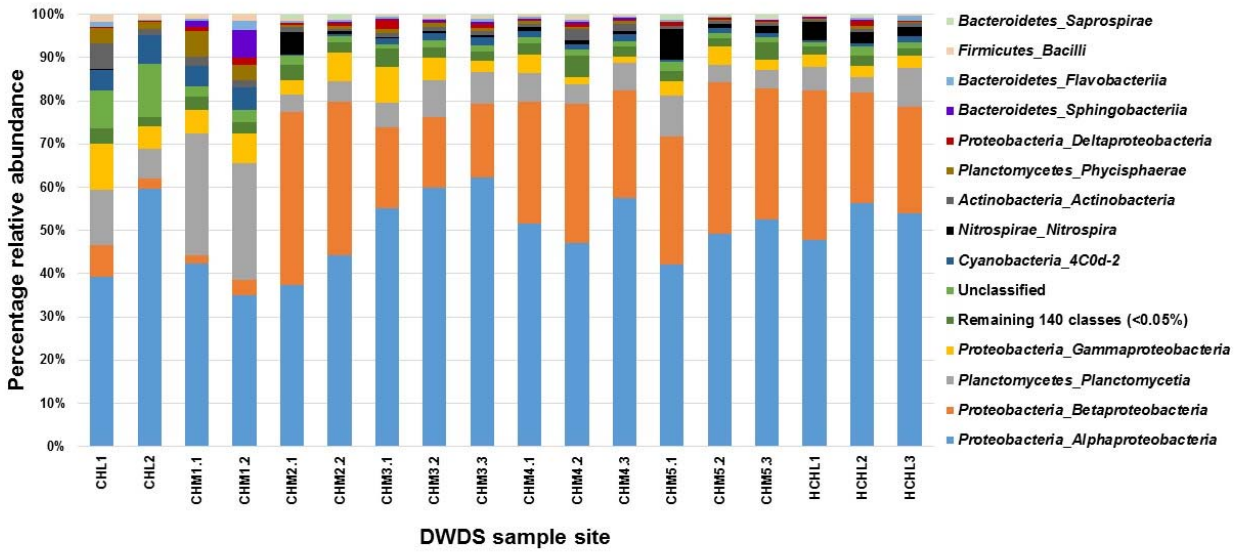

Figure 2. Class-level relative abundances of all bacterial sequences detected across the duration of the study at each DWDS sample site. The top thirteen most abundant bacterial classes are shown with the remaining 140 (constituting < 0.05% of the total abundance) grouped as a single group. Classes together with the phylum (phylum_class) they belong to are shown in the legend on the right.

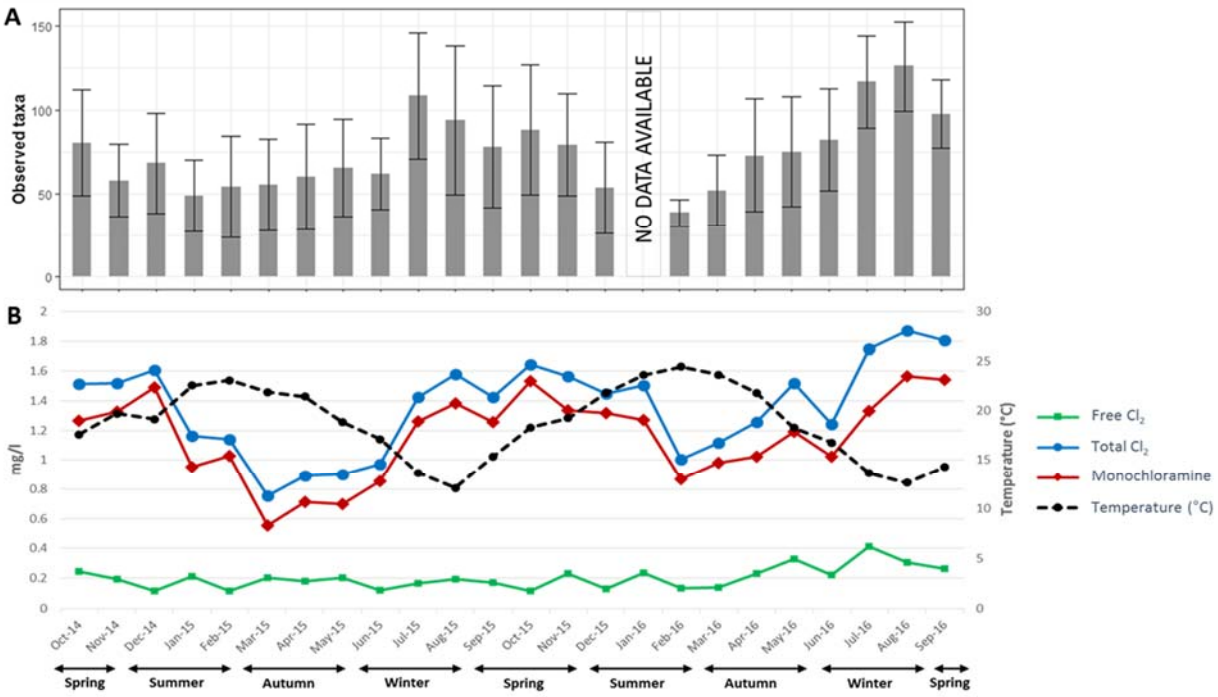

Figure 3. Temporal change in richness (observed taxa) averaged across all sample locations for which chemical data were available (i.e. CHL2, CHM1 – 4, CHM5.3 and HCHL1 – 3) for each month (A), correlated with average temperature (dashed black line) and average concentrations of disinfectant residuals (i.e., free chlorine [green squares], total chlorine [blue circles] and monochloramine [red diamonds]) over the duration of the study (B). Error bars represent the standard deviation in observed taxa across all sample sites within each month.

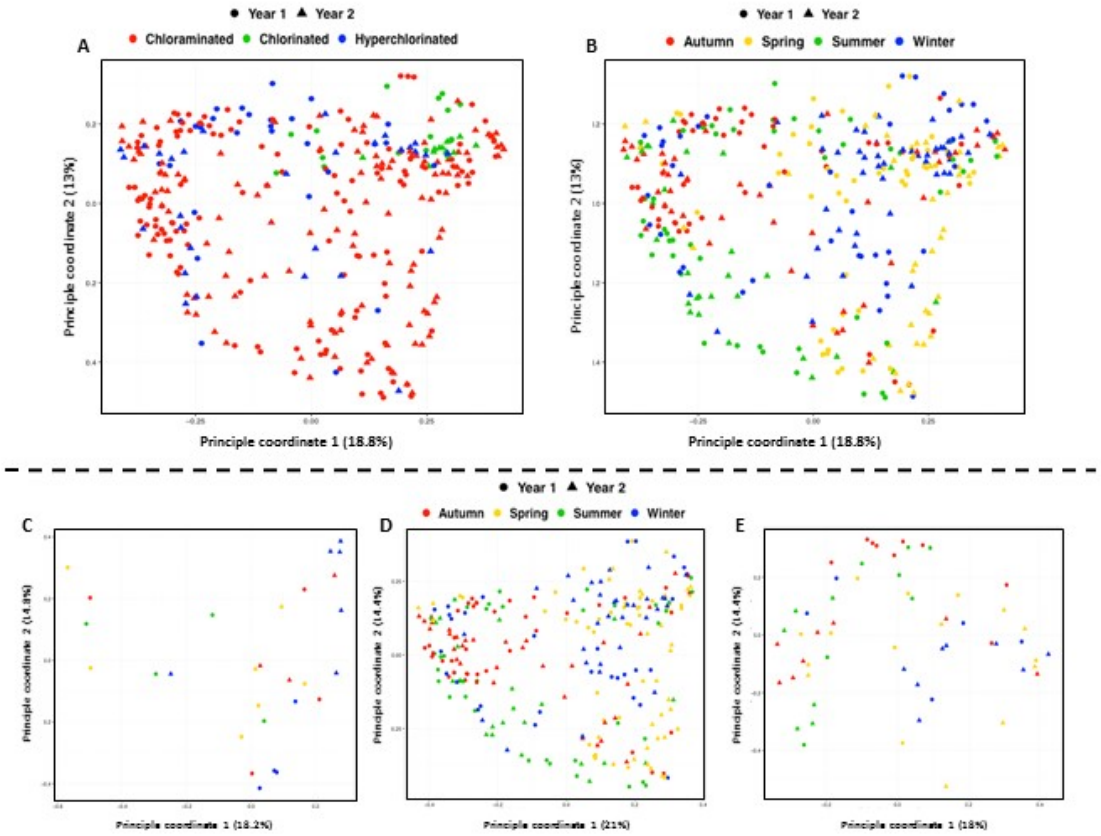

Figure 4. Principal-coordinate analyses plots showing the spatial and temporal variability of the bacterial community structure within the DWDS using Bray-Curtis dissimilarities. Spatial grouping is shown in plot (A) where data points are coloured based on disinfection strategy and shaped based on year. Temporal grouping are shown in plot (B) where data points are coloured based on season and shaped based on year. Colour and shapes are indicated in the legends on the top of both plots. The three lower plots indicate the temporal groupings within the three different disinfection sections, i.e. chlorinated (C), chloraminated (D) and hypochlorite (E). These three plots are coloured by season and shaped based on year, shown in the legend on the top of the plot D.

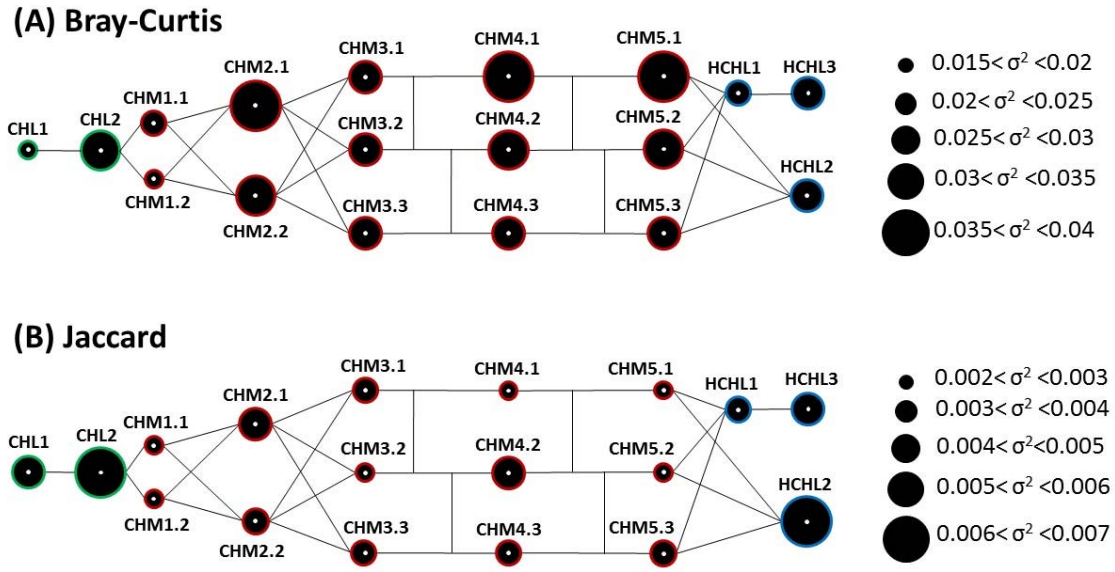

Figure 5. A schematic following the layout of the DWDS showing the extent of temporal variation at each sample site. White dots at the centre of each circle represent the median of all pairwise Bray-Curtis dissimilarity distances (A) and Jaccard distances (B) within each sample site over the duration of the study. Sizes of the black circles indicate the extent of temporal variance at each sample site. The extent of temporal variance is indicated in the legend on the right of the figure. Sample sites are coloured according to disinfection strategy (chlorination [green], chloramination [red] and hypochlorination [blue]).

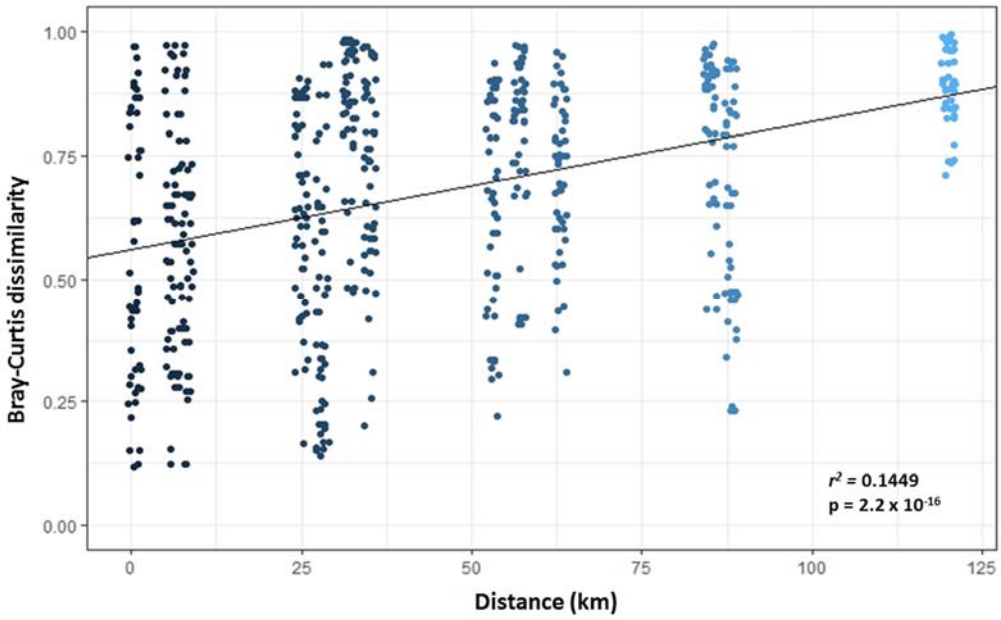

Figure 6. Distance decay features of the chloraminated section of the DWDS (CHM1 – CHM5) using pair wise structure-based Bray-Curtis distances. The line through the graph indicates the linear regression model. r^2 and significance values are shown on the graph.

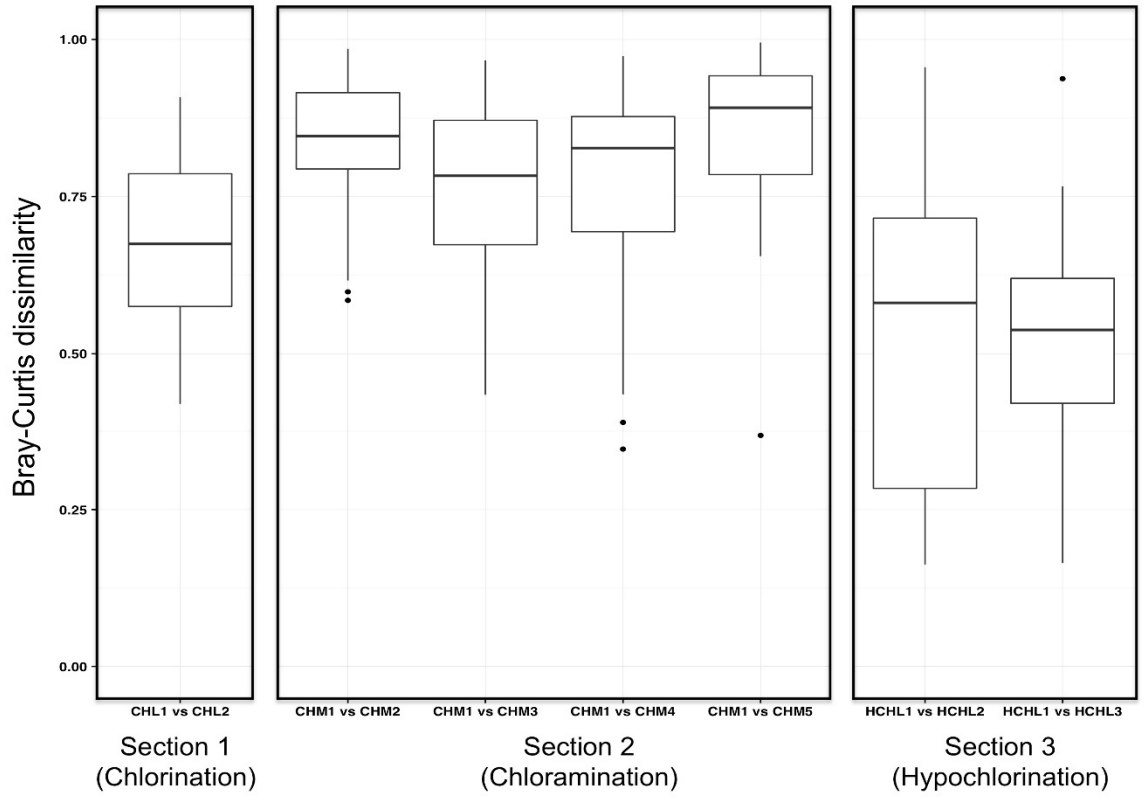

Figure 7. Comparisons of beta diversity distances between samples immediately after disinfection and with other samples within each disinfection section, were performed for all beta-diversity metrics. Pairwise distances were included from samples within a location from the same month.

Tables

Table 1: Outline and description of the multiple DWDS sample locations included in the study over the two-year study period and the number of samples sequenced for each sample site

	DWDS sample location	**Sample site***	**Number of samples sequenced**	**Sample location description**
1	CHL1	CHL1	15	Chlorinated water leaving the treatment plant
2	CHL2	CHL2	13	Chlorinated water entering boosting station
3	CHM1	CHM1.1	17	Chloraminated water leaving the boosting station
4		CHM1.2	14	Chloraminated water leaving the boosting station
5	CHM2	CHM2.1	22	Chloraminated reservoir
6		CHM2.2	20	Chloraminated reservoir
7	CHM3	CHM3.1	21	Chloraminated water leaving the pumping station
8		CHM3.2	20	Chloraminated water leaving the pumping station
9		CHM3.3	21	Chloraminated water leaving the pumping station
10	CHM4	CHM4.1	19	Chloraminated water pipeline
11		CHM4.2	21	Chloraminated water pipeline
12		CHM4.3	20	Chloraminated water pipeline
13	CHM5	CHM5.1	21	Chloraminated reservoir
14		CHM5.2	22	Chloraminated reservoir
15		CHM5.3	23	Chloraminated reservoir
16	HCHL1	HCHL1	21	Hypochlorinated water leaving boosting station
17	HCHL2	HCHL2	21	Hypochlorinated water leaving boosting station
18	HCHL3	HCHL3	17	Hypochlorinated water pipeline

* Some locations included multiple sample sites

Table 2: Percentage of total sequences, mean relative abundance and standard deviation of the most abundant OTUs (percentage of total sequences > 1%)

Operational taxonomic unit	**Taxonomic classification**	**Percentage of total sequences**	**Percentage MRA***	**SD***
OTU1	Genus: *Nitrosomonas*	18.49	14.97	18.94
OTU2	Order: *Rhizobiales*	14.7	14.45	19.92
OTU3	Order: *Rhizobiales*	12.47	12.11	14.07
OTU4	Genus: *Shingomonas*	9.72	9.16	10.02
OTU5	Family: *Gemmataceae*	3.72	4.81	7.54
OTU6	Genus: *Hyphomicobium*	1.98	1.8	3.34
OTU7	Genus: *Nitrospira*	1.83	1.68	3.74
OTU8	Class: *Betaproteobacteria* - SBla14	1.77	1.63	4.61
OTU9	Genus: *Planctomyces*	1.23	0.97	4.3

* MRA: Mean relative abundance

* SD: Standard deviation

Appendix A. Supplementary data

Supplementary Tables

Supplementary Table 1: Samples excluded due to failed sequencing

Sample site	Month	Season
CHL1	Nov-14	Spring
	Jan-15	Summer
	Feb-15	Summer
	Aug-15	Winter
	Dec-15	Summer
	Feb-16	Summer
	Mar-16	Autumn
	Sep-16	Spring
CHL2	Apr-15	Autumn
	May-15	Winter
	Jul-15	Winter
	Oct-15	Spring
	Nov-15	Spring
	Dec-15	Summer
	Feb-16	Summer
	Mar-16	Autumn
	May-16	Winter
	Sep-16	Spring
CHM1.1	Feb-15	Summer
	Jul-15	Winter
	Dec-15	Summer
	Feb-16	Summer
	Mar-16	Autumn
	Aug-16	Winter
CHM1.2	Apr-15	Autumn
	May-15	Winter
	Jul-15	Winter
	Sep-15	Spring
	Oct-15	Spring
	Nov-15	Spring
	Dec-15	Summer
	Feb-16	Summer
	Aug-16	Winter
CHM2.1	Apr-15	Autumn
CHM2.2	Jul-15	Winter
	Jul-16	Winter

	Sep-16	Spring
CHM3.1	Jun-15	Winter
	Jul-15	Winter
CHM3.2	Nov-15	Spring
	Dec-15	Summer
	Jul-16	Winter
CHM3.3	Aug-15	Winter
	Sep-15	Spring
CHM4.1	Aug-15	Winter
	Sep-15	Spring
	Apr-16	Autumn
	Jun-16	Winter
CHM4.2	Aug-15	Winter
	Sep-15	Spring
CHM4.3	Aug-15	Winter
	Sep-15	Spring
	Sep-16	Spring
CHM5.1	Jun-16	Winter
	Sep-16	Spring
CHM5.2	Aug-15	Winter
CHM5.3	-	-
HCHL1	Jul-15	Winter
	Aug-15	Winter
HCHL2	Feb-15	Summer
	Sep-16	Spring
HCHL3	Nov-14	Spring
	Feb-15	Summer
	Jun-15	Winter
	Jul-15	Winter
	Apr-16	Autumn
	Jun-16	Winter

Supplementary Table 3: Taxonomy of the subset of OTUs (95 OTUs) identified as the core community

OTU	Number of sequences per OTU	Phylum	Class	Order	Family	Genus	Species
Otu00001	1537994	*Proteobacteria*	*Betaproteobacteria*	*Nitrosomonadales*	*Nitrosomonadaceae*	*Nitrosomonas*	*Nitrosomonas oligotropha*
Otu00002	1223010	*Proteobacteria*	*Alphaproteobacteria*	*Rhizobiales*	unclassified	unclassified	unclassified
Otu00003	1037491	*Proteobacteria*	*Alphaproteobacteria*	*Rhizobiales*	unclassified	unclassified	unclassified
Otu00004	809246	*Proteobacteria*	*Alphaproteobacteria*	*Sphingomonadales*	*Sphingomonadaceae*	*Sphingomonas*	*Sphingomonas asaccharolytica*
Otu00005	310577	*Planctomycetes*	*Planctomycetia*	*Gemmatales*	*Gemmataceae*	unclassified	unclassified
Otu00006	164355	*Proteobacteria*	*Alphaproteobacteria*	*Rhizobiales*	*Hyphomicrobiaceae*	*Hyphomicrobium*	unclassified
Otu00007	152399	*Nitrospirae*	*Nitrospira*	*Nitrospirales*	*Nitrospiraceae*	*Nitrospira*	unclassified
Otu00008	147065	*Proteobacteria*	*Betaproteobacteria*	SBla14	unclassified	unclassified	unclassified
Otu00009	102091	*Planctomycetes*	*Planctomycetia*	*Planctomycetales*	*Planctomycetaceae*	*Planctomyces*	unclassified
Otu00010	74088	*Proteobacteria*	*Alphaproteobacteria*	*Rhizobiales*	*Hyphomicrobiaceae*	*Hyphomicrobium*	unclassified
Otu00011	71958	*Proteobacteria*	*Alphaproteobacteria*	*Rhizobiales*	*Hyphomicrobiaceae*	*Hyphomicrobium*	unclassified
Otu00012	71515	*Proteobacteria*	*Betaproteobacteria*	*Methylophilales*	*Methylophilaceae*	*Methylotenera*	*Methylotenera mobilis*
Otu00013	63553	*Proteobacteria*	*Betaproteobacteria*	*Gallionellales*	*Gallionellaceae*	*Gallionella*	unclassified
Otu00014	60813	*Proteobacteria*	*Betaproteobacteria*	unclassified	unclassified	unclassified	unclassified
Otu00015	58212	*Proteobacteria*	*Betaproteobacteria*	unclassified	unclassified	unclassified	unclassified
Otu00017	53380	*Proteobacteria*	*Alphaproteobacteria*	*Sphingomonadales*	*Sphingomonadaceae*	*Sphingobium*	*Sphingobium yanoikuyae*
Otu00018	51323	*Proteobacteria*	*Alphaproteobacteria*	*Rhodospirillales*	*Acetobacteraceae*	unclassified	unclassified
Otu00019	48399	*Cyanobacteria*	4C0d-2	MLE1-12	unclassified	unclassified	unclassified
Otu00020	47207	*Proteobacteria*	*Betaproteobacteria*	*Burkholderiales*	*Comamonadaceae*	unclassified	unclassified
Otu00021	46987	*Proteobacteria*	*Betaproteobacteria*	unclassified	unclassified	unclassified	unclassified
Otu00022	46057	*Planctomycetes*	*Planctomycetia*	*Planctomycetales*	*Planctomycetaceae*	*Planctomyces*	unclassified

Otu00023	42443	*Proteobacteria*	*Betaproteobacteria*	unclassified	unclassified	unclassified	unclassified
Otu00024	42069	*Proteobacteria*	*Alphaproteobacteria*	*Sphingomonadales*	*Erythrobacteraceae*	*Erythromicrobium*	*Erythromicrobium ramosum*
Otu00025	42021	*Proteobacteria*	*Alphaproteobacteria*	unclassified	unclassified	unclassified	unclassified
Otu00026	38929	*Proteobacteria*	*Alphaproteobacteria*	*Rhodobacterales*	*Rhodobacteraceae*	*Rhodobacter*	unclassified
Otu00027	38460	*Proteobacteria*	*Alphaproteobacteria*	*Rhodobacterales*	*Hyphomonadaceae*	unclassified	unclassified
Otu00028	38080	*Actinobacteria*	*Actinobacteria*	*Actinomycetales*	ACK-M1	unclassified	unclassified
Otu00029	37000	*Proteobacteria*	*Alphaproteobacteria*	unclassified	unclassified	unclassified	unclassified
Otu00030	35315	*Proteobacteria*	*Betaproteobacteria*	*Burkholderiales*	*Comamonadaceae*	*Acidovorax*	unclassified
Otu00031	33238	*Proteobacteria*	*Alphaproteobacteria*	*Caulobacterales*	*Caulobacteraceae*	*Mycoplana*	unclassified
Otu00032	32369	*Planctomycetes*	*Planctomycetia*	*Pirellulales*	*Pirellulaceae*	unclassified	unclassified
Otu00033	32048	*Planctomycetes*	*Phycisphaerae*	*Phycisphaerales*	unclassified	unclassified	unclassified
Otu00034	31501	unclassified	unclassified	unclassified	unclassified	unclassified	unclassified
Otu00035	30663	*Proteobacteria*	*Alphaproteobacteria*	*Sphingomonadales*	*Sphingomonadaceae*	unclassified	unclassified
Otu00037	29158	*Proteobacteria*	*Alphaproteobacteria*	*Rhizobiales*	*Bradyrhizobiaceae*	unclassified	unclassified
Otu00038	28463	*Planctomycetes*	*Phycisphaerae*	*Phycisphaerales*	unclassified	unclassified	unclassified
Otu00039	27107	*Planctomycetes*	*Planctomycetia*	*Gemmatales*	*Isosphaeraceae*	unclassified	unclassified
Otu00040	26689	*Proteobacteria*	*Gammaproteobacteria*	*Pseudomonadales*	*Pseudomonadaceae*	*Pseudomonas*	unclassified
Otu00041	25564	*Proteobacteria*	*Gammaproteobacteria*	*Enterobacteriales*	*Enterobacteriaceae*	*Escherichia*	*Escherichia coli*
Otu00042	25093	*Proteobacteria*	*Alphaproteobacteria*	*Rhizobiales*	unclassified	unclassified	unclassified
Otu00043	24912	*Bacteroidetes*	*[Saprospirae]*	*[Saprospirales]*	*Chitinophagaceae*	*Sediminibacterium*	unclassified
Otu00044	24849	*Proteobacteria*	*Betaproteobacteria*	*Burkholderiales*	*Comamonadaceae*	unclassified	unclassified
Otu00046	23570	*Proteobacteria*	*Alphaproteobacteria*	*Rhizobiales*	*Hyphomicrobiaceae*	*Hyphomicrobium*	unclassified
Otu00047	23033	*Proteobacteria*	*Alphaproteobacteria*	*Rhodospirillales*	*Rhodospirillaceae*	*Reyranella*	*Reyranella massiliensis*
Otu00048	22471	*Proteobacteria*	*Betaproteobacteria*	*Gallionellales*	*Gallionellaceae*	*Gallionella*	unclassified
Otu00049	22436	*Proteobacteria*	*Gammaproteobacteria*	unclassified	unclassified	unclassified	unclassified
Otu00050	21022	*Proteobacteria*	*Gammaproteobacteria*	*Alteromonadales*	*[Chromatiaceae]*	*Rheinheimera*	unclassified

Otu00051	19869	*Acidobacteria*	*Holophagae*	*Holophagales*	*Holophagaceae*	unclassified	unclassified
Otu00052	19310	*Cyanobacteria*	4C0d-2	MLE1-12	unclassified	unclassified	unclassified
Otu00053	17669	*Proteobacteria*	*Alphaproteobacteria*	*Rhizobiales*	unclassified	unclassified	unclassified
Otu00054	16870	*Proteobacteria*	*Betaproteobacteria*	*Rhodocyclales*	*Rhodocyclaceae*	*Sulfuritalea*	unclassified
Otu00055	16701	*Proteobacteria*	*Alphaproteobacteria*	*Sphingomonadales*	*Sphingomonadaceae*	*Novosphingobium*	*Novosphingobium stygium*
Otu00056	16690	*Cyanobacteria*	4C0d-2	MLE1-12	unclassified	unclassified	unclassified
Otu00057	16405	*Crenarchaeota*	*Thaumarchaeota*	*Cenarchaeales*	*Cenarchaeaceae*	unclassified	unclassified
Otu00058	15938	*Proteobacteria*	*Alphaproteobacteria*	unclassified	unclassified	unclassified	unclassified
Otu00059	15266	*Proteobacteria*	*Betaproteobacteria*	*Rhodocyclales*	*Rhodocyclaceae*	*Rhodocyclus*	unclassified
Otu00060	15064	*Proteobacteria*	*Alphaproteobacteria*	*Sphingomonadales*	*Sphingomonadaceae*	unclassified	unclassified
Otu00061	14218	*Proteobacteria*	*Alphaproteobacteria*	*Rhodobacterales*	*Rhodobacteraceae*	*Rhodobacter*	unclassified
Otu00062	14203	*Proteobacteria*	*Alphaproteobacteria*	*Rhizobiales*	*Methylobacteriaceae*	*Magnetospirillum*	*Magnetospirillum magnetotacticum*
Otu00064	13980	*Proteobacteria*	*Deltaproteobacteria*	*Spirobacillales*	unclassified	unclassified	unclassified
Otu00065	12429	*Actinobacteria*	*Actinobacteria*	*Actinomycetales*	ACK-M1	unclassified	unclassified
Otu00066	12288	*Bacteroidetes*	*Flavobacteriia*	*Flavobacteriales*	*Flavobacteriaceae*	*Flavobacterium*	*Flavobacterium succinicans*
Otu00067	12288	*Proteobacteria*	*Gammaproteobacteria*	*Pseudomonadales*	*Pseudomonadaceae*	*Pseudomonas*	unclassified
Otu00068	12254	*Actinobacteria*	*Actinobacteria*	*Actinomycetales*	*Mycobacteriaceae*	*Mycobacterium*	unclassified
Otu00069	11817	*Proteobacteria*	*Gammaproteobacteria*	*Aeromonadales*	*Aeromonadaceae*	*Aeromonas*	unclassified
Otu00070	11755	*Proteobacteria*	*Alphaproteobacteria*	*Rhodospirillales*	*Acetobacteraceae*	unclassified	unclassified
Otu00071	11689	*Bacteroidetes*	*Sphingobacteriia*	*Sphingobacteriales*	*Sphingobacteriaceae*	*Pedobacter*	unclassified
Otu00072	11456	*Proteobacteria*	*Gammaproteobacteria*	*Alteromonadales*	*Alteromonadaceae*	*Cellvibrio*	unclassified
Otu00073	11122	*Proteobacteria*	*Betaproteobacteria*	*Nitrosomonadales*	*Nitrosomonadaceae*	unclassified	unclassified
Otu00074	10129	*Proteobacteria*	*Alphaproteobacteria*	unclassified	unclassified	unclassified	unclassified
Otu00076	10022	*Proteobacteria*	*Betaproteobacteria*	*Burkholderiales*	*Oxalobacteraceae*	*Ralstonia*	unclassified
Otu00077	9528	*Actinobacteria*	*Actinobacteria*	*Actinomycetales*	ACK-M1	unclassified	unclassified

Otu00082	8022	*Proteobacteria*	*Alphaproteobacteria*	*Rhodospirillales*	*Acetobacteraceae*	*Roseomonas*	*Roseomonas stagni*
Otu00083	8021	*Proteobacteria*	*Betaproteobacteria*	*Nitrosomonadales*	*Nitrosomonadaceae*	unclassified	unclassified
Otu00084	7807	*Firmicutes*	*Bacilli*	*Bacillales*	*Staphylococcaceae*	*Staphylococcus*	unclassified
Otu00085	7773	*Bacteroidetes*	*Cytophagia*	*Cytophagales*	*Cyclobacteriaceae*	*Algoriphagus*	*Algoriphagus aquatilis*
Otu00086	7597	*Proteobacteria*	*Betaproteobacteria*	*Burkholderiales*	*Oxalobacteraceae*	*Massilia*	unclassified
Otu00089	7368	*Cyanobacteria*	4C0d-2	MLE1-12	unclassified	unclassified	unclassified
Otu00090	7230	*Proteobacteria*	*Alphaproteobacteria*	*Rhizobiales*	unclassified	unclassified	unclassified
Otu00092	6903	*Firmicutes*	*Bacilli*	*Lactobacillales*	*Streptococcaceae*	*Streptococcus*	*Streptococcus infantis*
Otu00094	6389	*Proteobacteria*	*Alphaproteobacteria*	*Sphingomonadales*	*Sphingomonadaceae*	unclassified	unclassified
Otu00095	6361	*Proteobacteria*	*Betaproteobacteria*	*Gallionellales*	*Gallionellaceae*	*Gallionella*	unclassified
Otu00096	5934	*Proteobacteria*	*Deltaproteobacteria*	*Desulfobacterales*	*Desulfobulbaceae*	unclassified	unclassified
Otu00097	5867	*Proteobacteria*	unclassified	unclassified	unclassified	unclassified	unclassified
Otu00099	5812	*Proteobacteria*	*Betaproteobacteria*	*Gallionellales*	*Gallionellaceae*	*Gallionella*	unclassified
Otu00100	5684	*Elusimicrobia*	*Elusimicrobia*	*Elusimicrobiales*	unclassified	unclassified	unclassified
Otu00104	5595	*Planctomycetes*	*Planctomycetia*	*Planctomycetales*	*Planctomycetaceae*	*Planctomyces*	unclassified
Otu00106	5197	*Bacteroidetes*	*Flavobacteriia*	*Flavobacteriales*	*Flavobacteriaceae*	*Flavobacterium*	unclassified
Otu00109	5004	unclassified	unclassified	unclassified	unclassified	unclassified	unclassified
Otu00110	4964	*Cyanobacteria*	4C0d-2	MLE1-12	unclassified	unclassified	unclassified
Otu00111	4862	*Proteobacteria*	*Alphaproteobacteria*	*Rhodospirillales*	*Acetobacteraceae*	unclassified	unclassified
Otu00115	4625	*Proteobacteria*	*Alphaproteobacteria*	*Sphingomonadales*	unclassified	unclassified	unclassified
Otu00121	3993	*Chlorobi*	*Ignavibacteria*	*Ignavibacteriales*	*[Melioribacteraceae]*	unclassified	unclassified
Otu00135	3317	*Cyanobacteria*	4C0d-2	MLE1-12	unclassified	unclassified	unclassified
Otu00137	3194	unclassified	unclassified	unclassified	unclassified	unclassified	unclassified

Supplementary Table 3: Phylum level classification of sequences within each sampling location over the duration of the study shown as relative abundances (%). The phylum *Proteobacteria* is divided into its respective classes

		CHL1	CHL2	CHM1	CHM2	CHM3	CHM4	CHM5	HCHL 1	HCHL 2	HCHL 3
Proteobacteria	***Alphaproteobacteria***	39.24	59.72	38.66	40.78	59.12	52.03	47.99	47.74	56.31	54.00
	Betaproteobacteria	7.33	2.27	2.70	37.74	17.38	28.46	31.63	34.60	25.49	24.57
	Deltaproteobacteria	0.25	0.31	1.30	0.74	1.09	0.50	0.50	0.37	1.20	0.26
	Epsilonproteobacteria	<0.01	<0.01	0.02419 8	0	0	<0.01	<0.01	<0.01	<0.01	0
	Gammaproteobacteria	10.69	5.30	6.26	5.12	5.33	2.33	3.44	2.82	2.70	2.94
	Unclassified Proteobacteria	1.95	4.19	0.85	0.38	0.24	0.29	0.43	0.23	0.87	0.29
	Planctomycetes	16.01	8.53	32.44	4.82	8.12	6.56	6.22	5.81	4.27	9.38
	Bacteroidetes	1.81	0.75	5.98	2.10	1.83	1.68	2.14	0.92	1.75	1.36
	Cyanobacteria	5.20	6.83	5.23	0.45	1.70	1.50	0.78	0.52	0.76	1.46
	unclassified	6.61	7.94	1.65	1.13	0.91	0.88	0.77	0.51	0.86	0.99
	Nitrospirae	0.17	0.04	0.03	2.86	0.44	0.85	3.30	4.11	2.73	2.03
	Actinobacteria	6.47	1.30	2.11	1.11	1.03	1.82	0.69	0.64	0.85	0.95
	Firmicutes	1.99	2.29	1.77	0.50	0.58	0.55	0.19	0.20	0.48	0.44
	Acidobacteria	1.16	0.14	0.45	0.77	0.73	0.90	0.55	0.41	0.40	0.44
	Crenarchaeota	0.39	0.04	0.25	0.15	0.16	0.31	0.44	0.54	0.07	0.22
	Chlorobi	0.13	<0.01	<0.01	0.52	0.51	0.09	0.14	0.02	0.08	0.12
	Elusimicrobia	<0.01	0.03	0.01	0.20	0.08	0.55	0.07	0.02	0.42	0.15
	Verrucomicrobia	0.21	0.03	0.09	0.24	0.19	0.21	0.17	0.16	0.27	0.12
	Gemmatimonadetes	0.06	<0.01	0.03	0.14	0.10	0.12	0.20	0.07	0.07	0.02
	Chloroflexi	0.04	<0.01	0.03	0.11	0.11	0.05	0.06	0.06	0.13	0.05
	OD1	0.05	<0.01	0.01	0.03	0.04	0.06	0.05	0.04	0.06	0.03
	Fusobacteria	0.08	0.05	0.04	<0.01	0.22	0.06	<0.01	0	0.01	<0.01
	Chlamydiae	<0.01	<0.01	0.02	0.03	0.04	0.06	0.04	0.04	0.04	<0.01
	Spirochaetes	<0.01	0	0.01	0.01	0.04	0.07	0.08	<0.01	0.06	0.07
	OP3	0.06	<0.01	<0.01	0.01	0.07	0.02	0.01	0.01	<0.01	<0.01
	TM6	<0.01	<0.01	0.01	0.01	0.02	0.02	0.03	0.02	0.03	0.02
	NKB19	0	0	0.00	0.01	0.01	<0.01	0.05	0.11	<0.01	0.03
	SBR1093	<0.01	0.15	<0.01	0.00	<0.01	0.02	<0.01	<0.01	0	<0.01
	Armatimonadetes	0.01	0.02	0.01	<0.01	0.01	0.02	0.01	<0.01	<0.01	<0.01
	WPS-2	0	<0.01	0	<0.01	<0.01	0	0.0129	<0.01	0.05	<0.01
	Euryarchaeota	<0.01	<0.01	0.02	<0.01	0.01	0.01	<0.01	<0.01	<0.01	<0.01
	[Thermi]	0.02	<0.01	0.01	<0.01	<0.01	<0.01	<0.01	<0.01	<0.01	<0.01
	ZB3	<0.01	0	0	<0.01	<0.01	<0.01	0.01	<0.01	<0.01	<0.01
	OP1	0	0	0	<0.01	0	0.03	<0.01	<0.01	<0.01	<0.01
	GN02	0	<0.01	0	<0.01	<0.01	<0.01	0.01	<0.01	<0.01	<0.01
	GN04	<0.01	0	0	<0.01	0.01	<0.01	0	<0.01	<0.01	<0.01
	TM7	0.01	<0.01	0.00	<0.01	<0.01	<0.01	<0.01	<0.01	<0.01	<0.01
	PAUC34f	<0.01	0	0	<0.01	<0.01	<0.01	0.01	0	<0.01	<0.01
	[Parvarchaeota]	<0.01	0	0	<0.01	<0.01	<0.01	<0.01	<0.01	<0.01	<0.01
	GOUTA4	0	0	0	0	0.01	0	0	0	0	0.01
	WS3	0	0	0	<0.01	<0.01	<0.01	<0.01	<0.01	0.01	<0.01
	NC10	0	0	0	0	0.01	0	0	0	0	0
	Tenericutes	<0.01	0	<0.01	0	<0.01	0	0	0	<0.01	0
	FBP	0	0	0.01	0	0	0	0	0	0	0
	BRC1	0	0	0	0	0	<0.01	0	<0.01	<0.01	<0.01
	Synergistetes	0	0	0	0	0	0	0	<0.01	0	0
	OP11	0	0	0	0	0	0	0	<0.01	0	<0.01
	Lentisphaerae	<0.01	0	0	0	0	0	0	0	<0.01	0
	SR1	<0.01	0	0	0	0	0	0	0	0	0
	AncK6	<0.01	0	0	0	0	0	0	0	0	0
	Aquificae	0	0	0	0	0	0	0	0	0	0
	Caldithrix	0	0	0	0	0	0	0	0	0	0
	TPD-58	0	0	0	0	0	0	0	0	0	0

	Thermotogae	0	0	0	0	0	0	0	0	0	0
	Kazan-3B-28	0	0	0	0	0	0	0	0	0	0
	Fibrobacteres	0	0	0	0	0	0	0	0	<0.01	0
	WWE1	0	0	0	0	0	0	0	0	<0.01	0
	WS2	0	0	0	0	0	0	0	<0.01	0	0
	[Caldithrix]	0	0	0	0	0	0	0	0	0	0
	Caldiserica	0	0	0	0	0	0	0	0	0	0
	WS5	0	0	0	0	0	0	0	0	0	0
	AD3	0	0	0	0	0	0	0	0	0	0
	AC1	0	0	0	0	0	0	0	<0.01	0	0
	MVP-21	0	0	0	0	0	0	0	0	0	0
	OP8	0	0	0	0	0	0	0	0	0	0
	KSB3	0	0	0	0	0	0	0	0	0	0

Supplementary Table 4: The mean and standard deviation (SD) for temperature, chlorine (free Cl_2 and total Cl_2) and monochloramine residual data for all sample sites averaged for each month of sampling

		Free Cl_2 (mg/l)		Total Cl_2 (mg/l)		Monochloramine (mg/l)		Temperature (°C)	
Season	**Date**	**Mean**	**SD**	**Mean**	**SD**	**Mean**	**SD**	**Mean**	**SD**
Spring	Oct-14	0.25	0.37	1.51	0.77	1.27	0.83	17.60	1.41
Spring	Nov-14	0.19	0.24	1.52	0.64	1.33	0.74	19.71	1.03
Summer	Dec-14	0.11	0.21	1.61	0.40	1.49	0.52	19.15	3.15
Summer	Jan-15	0.21	0.29	1.16	0.63	0.95	0.76	22.56	1.70
Summer	Feb-15	0.11	0.17	1.14	0.82	1.03	0.86	23.07	0.91
Autumn	Mar-15	0.20	0.30	0.75	0.68	0.55	0.67	21.88	0.92
Autumn	Apr-15	0.18	0.41	0.89	0.79	0.71	0.76	21.45	2.47
Autumn	May-15	0.20	0.40	0.90	0.73	0.70	0.75	18.83	1.61
Winter	Jun-15	0.12	0.25	0.97	0.76	0.85	0.79	17.10	1.81
Winter	Jul-15	0.16	0.26	1.42	0.69	1.26	0.76	13.68	2.27
Winter	Aug-15	0.20	0.42	1.58	0.65	1.39	0.84	12.11	1.44
Spring	Sep-15	0.17	0.22	1.43	0.72	1.26	0.83	15.33	1.54
Spring	Oct-15	0.11	0.26	1.65	0.34	1.53	0.50	18.31	2.40
Spring	Nov-15	0.23	0.21	1.57	0.56	1.34	0.69	19.27	0.67
Summer	Dec-15	0.13	0.20	1.45	0.53	1.32	0.62	21.78	1.59
Summer	Jan-16	0.23	0.43	1.50	0.55	1.27	0.73	23.63	2.00
Summer	Feb-16	0.13	0.27	1.00	0.62	0.87	0.66	24.44	1.37
Autumn	Mar-16	0.14	0.29	1.12	0.70	0.98	0.75	23.64	0.98
Autumn	Apr-16	0.23	0.34	1.26	0.60	1.02	0.78	21.84	0.88
Autumn	May-16	0.33	0.45	1.52	0.39	1.19	0.73	18.29	1.74
Winter	Jun-16	0.22	0.33	1.24	0.69	1.02	0.81	16.76	1.60
Winter	Jul-16	0.42	0.42	1.75	0.52	1.33	0.65	13.62	1.64
Winter	Aug-16	0.31	0.45	1.87	0.22	1.57	0.60	12.63	1.54
Spring	Sep-16	0.26	0.30	1.81	0.34	1.54	0.62	14.25	1.18

Supplementary Table 5: Summary of PERMANOVA results indicating the influence of temporal and spatial grouping on the overall bacterial community membership and structure within the entire DWDS (CHL1 – HCHL3)

Membership based metrics

Jaccard distance

	Degrees of freedom	Sum of squares	Mean of squares	F.Model	R2	Pr(>F)
Season overall	3	6.296	2.09866	6.5431	0.04804	0.001***
Sample location	9	14.017	1.55748	4.8558	0.10695	0.001***
Season overall: Sample location	27	11.965	0.44313	1.3816	0.09129	0.001***
Residuals	308	98.79	0.32075		0.75373	
Total	347	131.068			1	

Unweighted UniFrac distance

	Degrees of freedom	Sum of squares	Mean of squares	F.Model	R2	Pr(>F)
Season overall	3	3.255	1.08487	4.124	0.03156	0.001***
Sample location	9	11.073	1.23035	4.677	0.10739	0.001***
Season overall: Sample location	27	7.759	0.28735	1.0923	0.07525	0.004**
Residuals	308	81.023	0.26306		0.7858	
Total	347	103.109			1	

Structure based metrics

Bray-Curtis distance

	Degrees of freedom	Sum of squares	Mean of squares	F.Model	R2	Pr(>F)
Season overall	3	6.827	2.27566	9.2913	0.06276	0.001***
Sample location	9	16.343	1.81593	7.4142	0.15025	0.001***
Season overall: Sample location	27	10.166	0.3765	1.5372	0.09346	0.001***
Residuals	308	75.437	0.24492		0.69353	
Total	347	108.773			1	

Weighted UniFrac distance

	Degrees of freedom	Sum of squares	Mean of squares	F.Model	R2	Pr(>F)
Season overall	3	4.973	1.65776	11.9069	0.07271	0.001***
Sample location	9	14.18	1.57551	11.3162	0.20732	0.001***
Season overall: Sample location	27	6.361	0.23559	1.6921	0.093	0.001***
Residuals	308	42.882	0.13923		0.62697	
Total	347	68.396			1	

Significance codes: 0 '***' 0.001 '**' 0.01 '*' 0.05 '.' 0.1 ' ' 1

Supplementary Table 6: Summary of PERMANOVA results indicating the influence of temporal and spatial grouping on bacterial community membership and structure within the chlorinated section of the DWDS (Section 1) (CHL1 – CHL2)

Membership based metrics

Jaccard distance

	Degrees of freedom	Sum of squares	Mean of squares	F.Model	R2	Pr(>F)
Yearly seasons	6	2.496	0.416	1.40387	0.28605	0.001***
Sample site	1	0.3082	0.30816	1.03996	0.03532	0.422
Yearly seasons: Sample site	6	1.773	0.29549	0.99721	0.20319	0.499
Residuals	14	4.1485	0.29632		0.47544	
Total	27	8.7256			1	

Unweighted UniFrac distance

	Degrees of freedom	Sum of squares	Mean of squares	F.Model	R2	Pr(>F)
Yearly seasons	6	2.1539	0.35899	1.4456	0.28803	0.001***
Sample site	1	0.3343	0.33433	1.3463	0.04471	0.035*
Yearly seasons: Sample site	6	1.5133	0.25222	1.0157	0.20237	0.424
Residuals	14	3.4766	0.24833		0.4649	
Total	27	7.4782			1	

Structure based metrics

Bray-Curtis distance

	Degrees of freedom	Sum of squares	Mean of squares	F.Model	R2	Pr(>F)
Yearly seasons	6	3.5591	0.59318	2.1932	0.35445	0.001***
Sample site	1	0.5112	0.5112	1.8901	0.05091	0.022*
Yearly seasons: Sample site	6	2.1844	0.36407	1.3461	0.21755	0.028*
Residuals	14	3.7864	0.27046		0.37709	
Total	27	10.0411			1	

Weighted UniFrac distance

	Degrees of freedom	Sum of squares	Mean of squares	F.Model	R2	Pr(>F)
Yearly seasons	6	2.3552	0.39253	2.7447	0.40548	0.001***
Sample site	1	0.2985	0.29849	2.0871	0.05139	0.048*
Yearly seasons: Sample site	6	1.1526	0.19209	1.3432	0.19843	0.095.
Residuals	14	2.0022	0.14301		0.3447	
Total	27	5.8084			1	

Significance codes: 0 '***' 0.001 '**' 0.01 '*' 0.05 '.' 0.1 ' ' 1

Supplementary Table 7: Summary of PERMANOVA results indicating the influence of temporal and spatial grouping on bacterial community membership and structure within the chloraminated section of the DWDS (section 2) (CHM1 – CHM5)

Membership based metrics						
Jaccard distance						
	Degrees of freedom	**Sum of squares**	**Mean of squares**	**F.Model**	**R2**	**Pr(>F)**
Yearly seasons	8	2.697	0.33713	1.0881	0.03196	0.092.
Sample site	12	5.303	0.44195	1.4264	0.06285	0.001***
Yearly seasons: Sample site	90	29.913	0.33236	1.0727	0.35446	0.004**
Residuals	150	46.476	0.30984		0.55073	
Total	260	84.389			1	
Unweighted UniFrac distance						
	Degrees of freedom	**Sum of squares**	**Mean of squares**	**F.Model**	**R2**	**Pr(>F)**
Yearly seasons	8	2.321	0.29012	1.0904	0.032	0.084.
Sample site	12	4.446	0.37049	1.3925	0.0613	0.001***
Yearly seasons: Sample site	90	25.846	0.28717	1.0793	0.35638	0.004**
Residuals	150	39.91	0.26607		0.55031	
Total	260	72.522			1	
Structure based metrics						
Bray-Curtis distance						
	Degrees of freedom	**Sum of squares**	**Mean of squares**	**F.Model**	**R2**	**Pr(>F)**
Yearly seasons	8	4.649	0.58114	2.19045	0.06422	0.001***
Sample site	12	2.774	0.23119	0.87141	0.03832	0.805
Yearly seasons: Sample site	90	25.179	0.27977	1.0545	0.34778	0.194
Residuals	150	39.796	0.26531		0.54968	
Total	260	72.398			1	
Weighted UniFrac distance						
	Degrees of freedom	**Sum of squares**	**Mean of squares**	**F.Model**	**R2**	**Pr(>F)**
Yearly seasons	8	2.974	0.37179	2.41979	0.07175	0.001***
Sample site	12	0.942	0.07848	0.51076	0.02272	0.996
Yearly seasons: Sample site	90	14.492	0.16102	1.048	0.34958	0.296
Residuals	150	23.047	0.15365		0.55595	
Total	260	41.455			1	

Significance codes: 0 '***' 0.001 '**' 0.01 '*' 0.05 '.' 0.1 ' ' 1

Supplementary Table 8: Summary of PERMANOVA results indicating the influence of temporal and spatial grouping on bacterial community membership and structure within the hypochlorinated section (section 3) (HCHL1 – HCHL3)

Membership based metrics

Jaccard distance

	Degrees of freedom	Sum of squares	Mean of squares	F.Model	R2	Pr(>F)
Yearly seasons	8	3.3931	0.42414	1.28402	0.17253	0.013*
Sample site	2	1.1463	0.57317	1.73522	0.05829	0.002**
Yearly seasons: Sample site	15	4.2263	0.28176	0.85299	0.2149	0.977
Residuals	33	10.9005	0.33032		0.55427	
Total	58	19.6663			1	

Unweighted UniFrac distance

	Degrees of freedom	Sum of squares	Mean of squares	F.Model	R2	Pr(>F)
Yearly seasons	8	2.4068	0.30086	0.93813	0.13204	0.86
Sample site	2	0.6696	0.3348	1.04396	0.03673	0.341
Yearly seasons: Sample site	15	4.569	0.3046	0.94981	0.25065	0.887
Residuals	33	10.583	0.3207		0.58058	
Total	58	18.2285			1	

Structure based metrics

Bray-Curtis distance

	Degrees of freedom	Sum of squares	Mean of squares	F.Model	R2	Pr(>F)
Yearly seasons	8	3.8918	0.48647	1.8854	0.22227	0.001***
Sample site	2	2.0915	1.04577	4.0531	0.11945	0.001***
Yearly seasons: Sample site	15	3.0112	0.20075	0.778	0.17198	0.96
Residuals	33	8.5145	0.25802		0.48629	
Total	58	17.509			1	

Weighted UniFrac distance

	Degrees of freedom	Sum of squares	Mean of squares	F.Model	R2	Pr(>F)
Yearly seasons	8	1.9022	0.23777	1.7753	0.20321	0.002**
Sample site	2	1.0361	0.51807	3.8681	0.11069	0.001***
Yearly seasons: Sample site	15	2.0028	0.13352	0.9969	0.21395	0.503
Residuals	33	4.4198	0.13393		0.47215	
Total	58	9.3609			1	

Significance codes: 0 '***' 0.001 '**' 0.01 '*' 0.05 '.' 0.1 ' ' 1

Supplementary Figures

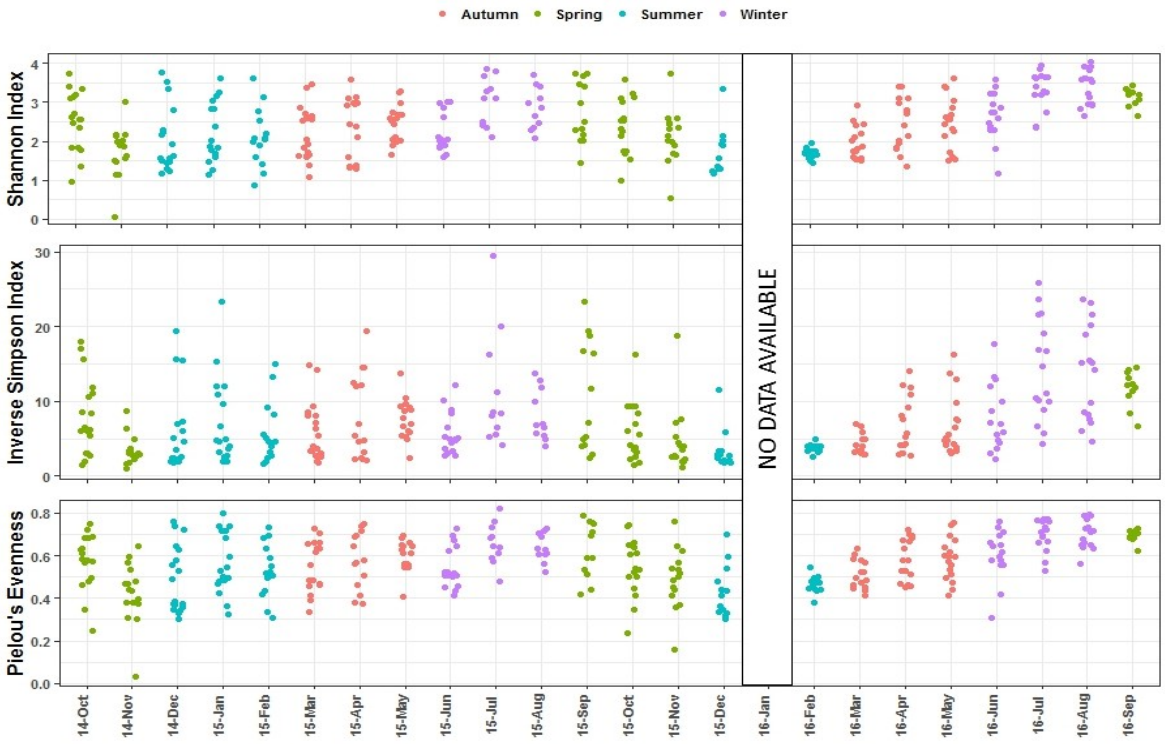

Supplementary Figure 1: Temporal changes in diversity (Shannon Index and Inverse Simpson Index) and evenness (Pielou's evenness) averaged across all sampling locations for each month. Points represent all sample sites collected for each month. Months are coloured based on season indicated in the legend above.

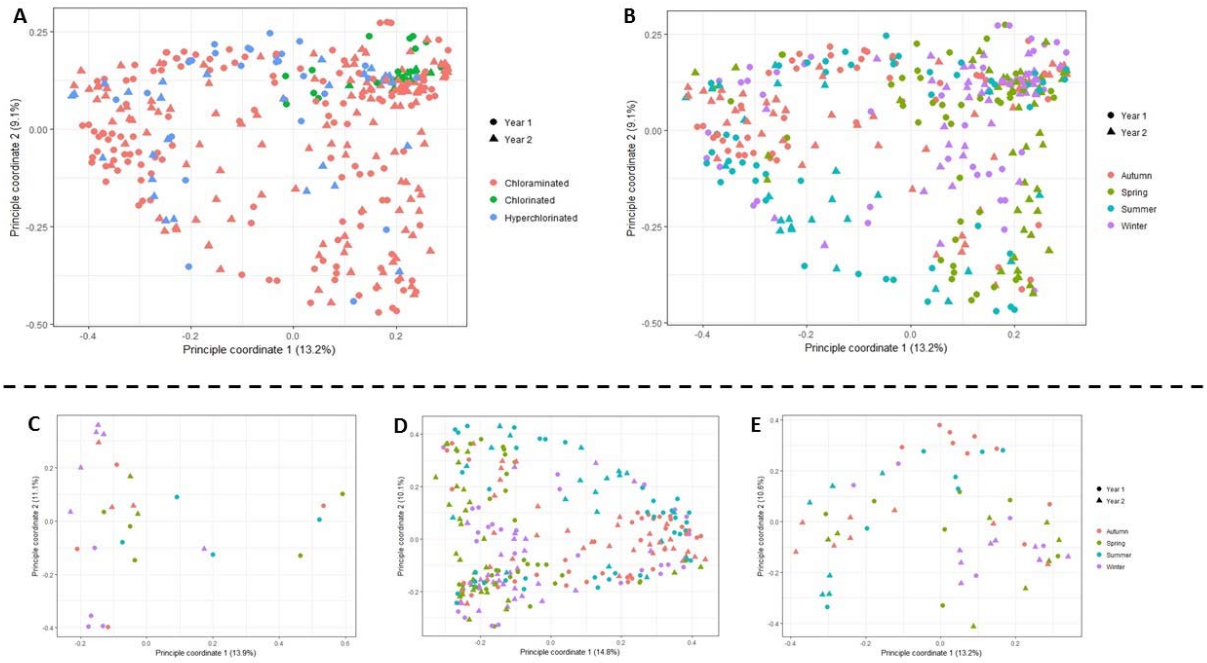

Supplementary Figure 2: Principal-coordinate bipolts showing the spatial and temporal variability of the bacterial community membership within the DWDS using Jaccard dissimilarities distances. Spatial grouping are shown in plot (A) where data points are coloured based on disinfection strategy used and shaped based on year. Temporal grouping are shown in plot (B) where data points are coloured based on season and shaped based on year. Colour and shapes are indicated in the legends on the right of both plots. The three lower plots indicate the temporal groupings within the three sections using different disinfection strategies i.e. chlorinated (C), chloraminated (D) and hyperchlorite (E). These three plots are coloured by season and shaped based on year, shown in the legend on the right of the plot E.

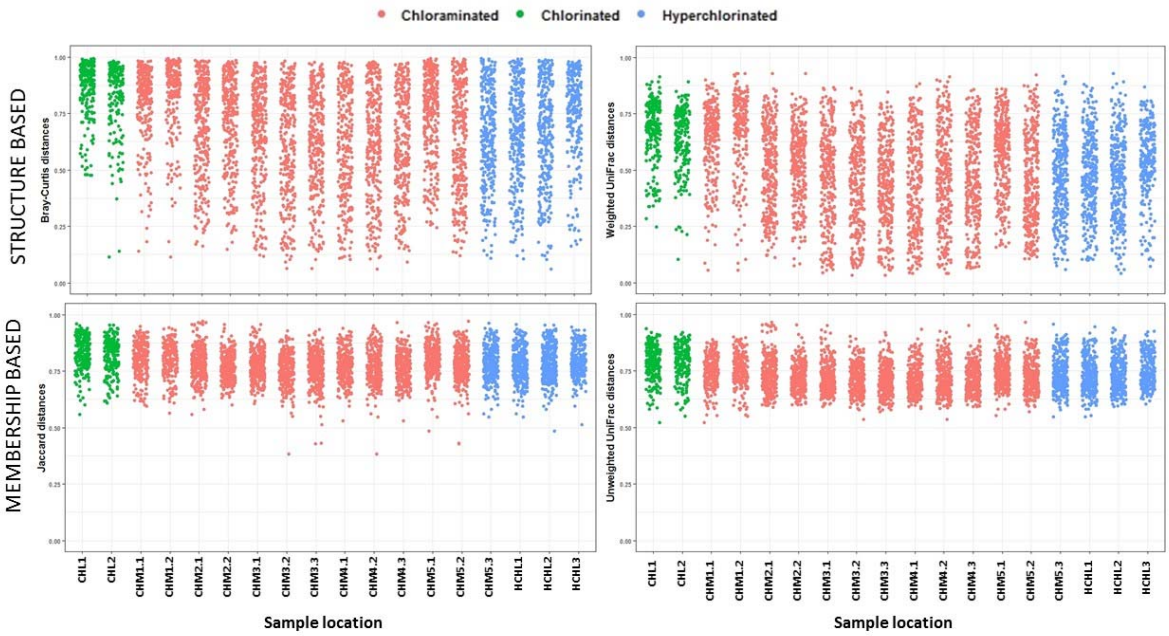

Supplementary Figure 3: The extent of temporal variation in both the bacterial community structure and membership within each sample site over the duration of the study using pairwise distances of all Beta diversity metrics.

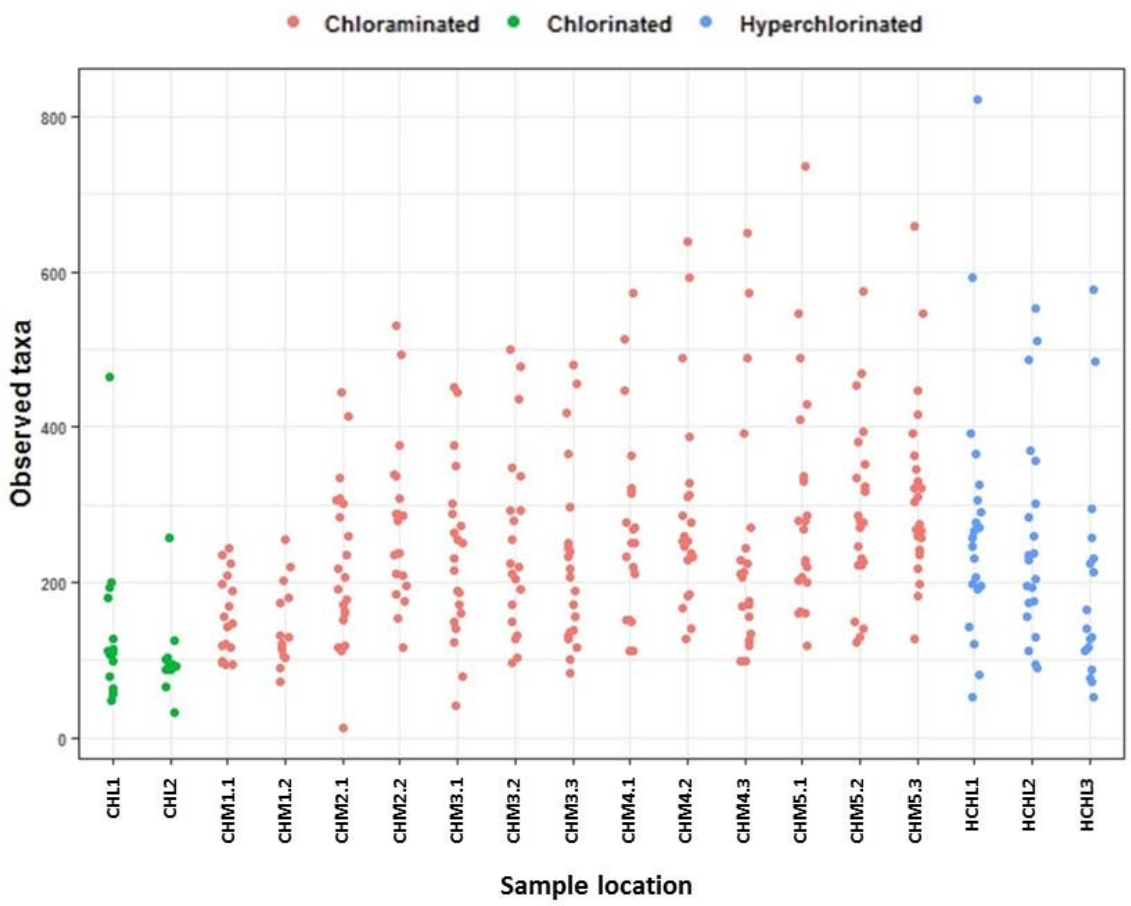

Supplementary Figure 4: Spatial changes in richness (observed taxa) across the DWDS. Points represent each month over 2-years at each sample site. Sample sites are coloured based on disinfection strategy indicated in the legend on the right.

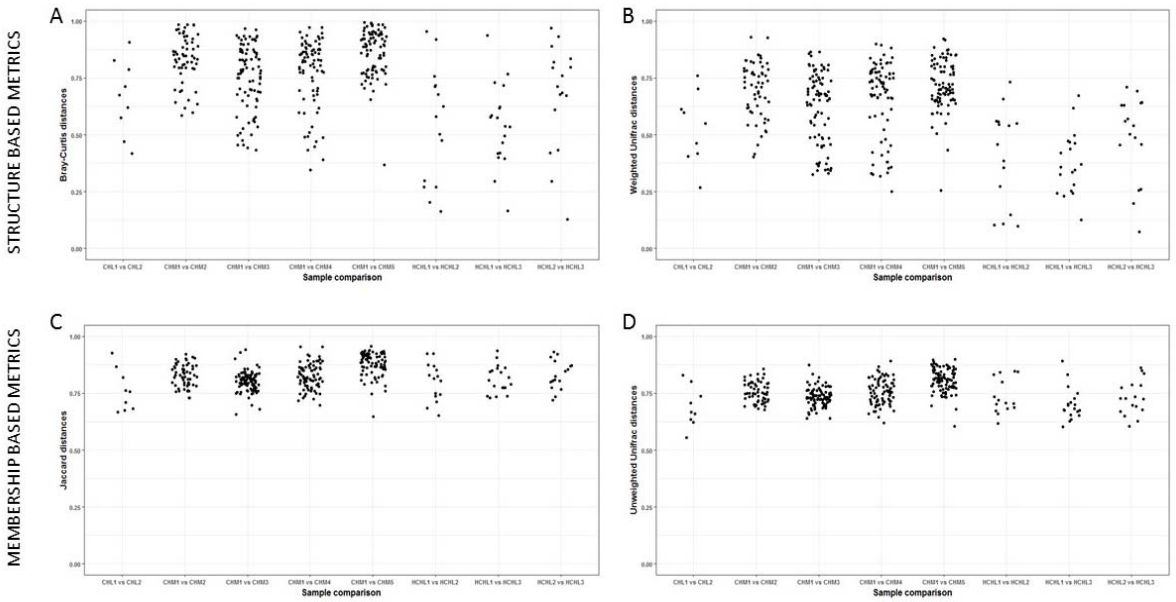

Supplementary Figure 5: Pair wise beta-diversity distances (structure based metrics: Bray-Curtis [A] and weighted UniFrac [B]; membership based metrics: Jaccard [C] and unweighted UniFrac [D]) between DWDS sample locations within each disinfection section. Comparisons include the first sample after one of the three disinfections compared to all other samples within each disinfection section.